

**SINGLE MODE D-SHAPE OPTICAL FIBER STRUCTURES AS 2D  
MATERIAL SATURABLE ABSORBER FOR PULSED FIBER  
LASER GENERATION**

**NG YI HEN**



**UNIVERSITI TEKNIKAL MALAYSIA MELAKA**

**SINGLE MODE D-SHAPE OPTICAL FIBER STRUCTURES AS  
2D LIGHT MATERIAL SATURABLE ABSORBER FOR  
PULSED FIBER LASER GENERATION**

**NG YI HEN**

**This report is submitted in partial fulfilment of the requirements  
for the degree of Bachelor of Electronic Engineering with Honours**



**Faculty of Electronics and Computer Technology and  
Engineering**  
**UNIVERSITI** **Universiti Teknikal Malaysia Melaka** **KA**

**2024**

**BORANG PENGESAHAN STATUS LAPORAN  
PROJEK SARJANA MUDA II**

Tajuk Projek : **Single Mode D-shape Optical Fiber Structures as 2D Light  
Material Saturable Absorber for Pulsed Fiber Laser Generation**  
Sesi Pengajian : 2022/2023

Saya NG YI HEN mengaku membenarkan laporan Projek Sarjana Muda ini disimpan di Perpustakaan dengan syarat-syarat kegunaan seperti berikut:

1. Laporan adalah hakmilik Universiti Teknikal Malaysia Melaka.
2. Perpustakaan dibenarkan membuat salinan untuk tujuan pengajian sahaja.
3. Perpustakaan dibenarkan membuat salinan laporan ini sebagai bahan pertukaran antara institusi pengajian tinggi.
4. Sila tandakan (✓):

**SULIT\***

(Mengandungi maklumat yang berdarjah keselamatan atau kepentingan Malaysia seperti yang termaktub di dalam AKTA RAHSIA RASMI 1972)

**TERHAD\***

(Mengandungi maklumat terhad yang telah ditentukan oleh organisasi/badan di mana penyelidikan dijalankan.)

**TIDAK TERHAD**

Disahkan oleh:



(TANDATANGAN PENULIS)



(COP DAN TANDATANGAN PENYELIA)

Alamat Tetap: 34, Jalan Sahabat  
2, Taman Emas,  
86000 Kluang,  
Johor.

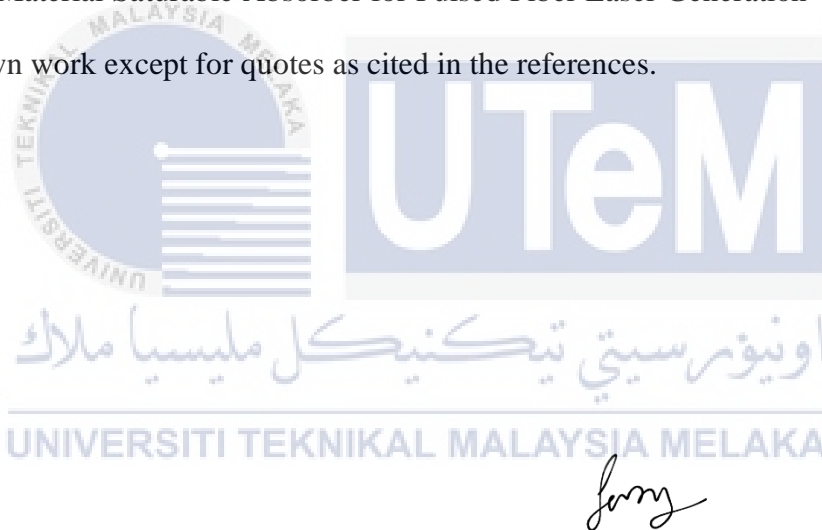
**IR. DR. ANAS BIN ABDUL LATIFF**  
Pensyarah Kanan  
Fakulti Teknologi Dan Kejuruteraan Elektronik Dan Komputer (FTKEK)  
Universiti Teknikal Malaysia Melaka (UTeM)

Tarikh : 11/1/2024

Tarikh : **11-JAN-2024**

## DECLARATION

I declare that this report entitled “Single Mode D-shape Optical Fiber Structures as 2D Light Material Saturable Absorber for Pulsed Fiber Laser Generation” is the result of my own work except for quotes as cited in the references.



Signature : .....

Author : Ng Yi Hen  
.....

Date : 11/1/2024  
.....

## APPROVAL

I hereby declare that I have read this thesis and in my opinion this thesis is sufficient in terms of scope and quality for the award of Bachelor of Electronic Engineering with Honours.



اونيورسيتي تنيكنيكل مليسيا ملاك  
Signature : 

UNIVERSITI TEKNIKAL MALAYSIA MELAKA

Supervisor Name : IR. DR. ANAS BIN ABDUL LATIFF

Date : **11-JAN-2024**

## DEDICATION

This project is dedicated to the pioneers in fiber optics, laser technology, and materials science, whose groundbreaking contributions paved the way for this exploration. It acknowledges the tireless efforts of researchers and scientists who delved into the intricacies of D-shaped fiber optics and saturable absorbers, pushing the boundaries of understanding. The dedication extends to my educators and mentors which are Dr Anas, Abang Aizat, and Kak Yana, whose guidance shaped inquisitive minds, fostering a passion for discovery. A heartfelt acknowledgment is extended to colleagues and collaborators which are Janzen and Ronald, whose diverse expertise enriched this project, creating an environment of shared knowledge. The support networks of friends and family, offering encouragement through challenges and celebrations during triumphs, are deeply appreciated. In tribute to the spirit of inquiry, pursuit of excellence, and collaborative ethos that propels scientific progress, this project stands as a testament to the collective human endeavour to explore the unknown in science and technology. Gratitude is expressed to all who contributed, fostering an environment where curiosity thrives and innovation flourishes.

## ABSTRACT

This project explores the transformative potential of utilizing MAX phase  $\text{Ti}_4\text{AlN}_3$  as a saturable absorber in the generation of pulsed fiber lasers. MAX phase materials, renowned for their unique combination of metallic and ceramic properties, present promising characteristics for saturable absorption. The focus on  $\text{Ti}_4\text{AlN}_3$  stems from its composition—four atoms of titanium, one of aluminium, and three of nitrogen—providing exceptional thermal stability, mechanical strength, and electrical conductivity. The study achieves a significant milestone in fabricating D-shaped optical fibers tailored for MAX phase incorporation. The meticulous process involves creating a MAX phase solution by blending polyvinyl alcohol (PVA) and  $\text{Ti}_4\text{AlN}_3$ , followed by depositing this solution onto polished D-shaped fibers, laying the foundation for inducing pulsed fiber laser generation. The project's methodology includes theoretical analyses, numerical simulations, and experimental characterizations to comprehensively evaluate  $\text{Ti}_4\text{AlN}_3$  as a saturable absorber. Employing a 2.4 m Erbium-doped fiber laser setup, the results demonstrate the feasibility and efficacy of  $\text{Ti}_4\text{AlN}_3$  in inducing Q-switched pulses, showcasing its potential for high-performance pulsed fiber lasers. This research not only contributes to advancing fiber laser technology but also opens avenues for applications in diverse

fields, ranging from industrial manufacturing to telecommunications and medical devices.





## ABSTRAK

*Projek ini meneroka potensi transformatif menggunakan fasa MAX  $Ti_4AlN_3$  sebagai penyerap tepu dalam penjanaan laser gentian berdenyut. Bahan fasa MAX, yang terkenal dengan gabungan unik sifat logam dan seramik, memberikan ciri-ciri yang menjanjikan untuk penyerapan tepu. Tumpuan pada  $Ti_4AlN_3$  berpunca daripada komposisinya—empat atom titanium, satu daripada aluminium dan tiga daripada nitrogen—menyediakan kestabilan haba yang luar biasa, kekuatan mekanikal dan kekonduksian elektrik. Kajian ini mencapai pencapaian penting dalam fabrikasi gentian optik berbentuk D yang disesuaikan untuk pemerbadanan fasa MAX. Proses yang teliti melibatkan penciptaan penyelesaian fasa MAX dengan mengadun polivinil alkohol (PVA) dan  $Ti_4AlN_3$ , diikuti dengan mendepositkan larutan ini pada gentian berbentuk D yang digilap, meletakkan asas untuk mendorong penjanaan laser gentian berdenyut. Metodologi projek termasuk analisis teori, simulasi berangka, dan pencirian eksperimen untuk menilai secara menyeluruh  $Ti_4AlN_3$  sebagai penyerap tepu. Menggunakan persediaan laser gentian dop Erbium 2.4 m, hasilnya menunjukkan kebolehlaksanaan dan keberkesanan  $Ti_4AlN_3$  dalam mendorong denyutan bertukar Q, mempamerkan potensinya untuk laser gentian berdenyut berprestasi tinggi. Penyelidikan ini bukan sahaja menyumbang kepada memajukan*

*teknologi laser gentian tetapi juga membuka ruang untuk aplikasi dalam pelbagai bidang, daripada pembuatan industri kepada telekomunikasi dan peranti perubatan.*



## ACKNOWLEDGEMENTS

This project has been a collective efforts, and I extend my sincere gratitude to all who contributed to its realization. Firstly, heartfelt thanks to the pioneers in fiber optics, laser technology, and materials science, whose groundbreaking work laid the foundation for this exploration. I express my deepest appreciation to the researchers and scientists whose dedication and expertise were instrumental in unravelling the complexities of D-shaped fiber optics and saturable absorbers. Your contributions have been invaluable in advancing our understanding of these critical components.

Special thanks to my mentors and educators which are Ir. Dr. Anas Bin Abdul Latiff and Abang Aizat for their guidance, wisdom, and unwavering support throughout this journey. Your mentorship has been a guiding light, shaping my approach to scientific inquiry. I am grateful to my colleagues and collaborators which are Janzen and Ronald for their diverse perspectives and collective efforts, which enriched the project and created a collaborative environment conducive to innovation. Last but not least, heartfelt appreciation goes to my friends and family whose support sustained me during the challenges and celebrated the milestones. Your encouragement was a driving force. In acknowledging these contributions, I recognize the collaborative

spirit that fuels scientific exploration, and I am indebted to each individual who played a role in bringing this project to fruition.



## TABLE OF CONTENTS

<b>Declaration</b>	
<b>Approval</b>	
<b>Dedication</b>	
<b>Abstract</b>	<b>i</b>
<b>Abstrak</b>	<b>iii</b>
<b>Acknowledgements</b>	<b>v</b>
<b>Table of Contents</b>	<b>vii</b>
<b>List of Figures</b>	<b>x</b>
<b>List of Tables</b>	<b>xii</b>
<b>List of Symbols and Abbreviations</b>	<b>xiii</b>
<b>CHAPTER 1 INTRODUCTION</b>	<b>14</b>
1.1 Background of Study	15
1.2 Problem Statement	16
1.3 Objectives	17
1.4 Scope	18
<b>CHAPTER 2 BACKGROUND STUDY</b>	<b>19</b>

2.1	Fiber lasers	20
2.1.1	Optical fibers	21
2.1.2	Single-mode fiber	22
2.1.3	Erbium doped fiber lasers	24
2.1.4	Passively Q-switched lasers	27
2.2	D-shaped optical fiber	30
2.3	Two-dimensional (2D) materials	31
2.4	Saturable absorber	33
2.4.1	MAX phase as saturable absorber	35
<b>CHAPTER 3 METHODOLOGY</b>		<b>41</b>
3.1	Fabrication of Saturable Absorber	42
3.1.1	Fabrication of D-shaped Fiber Optic	42
3.1.1.1	Insertion Loss of D-shaped Fiber	43
3.1.2	Preparation of MAX phase $Ti_4AlN_3$	45
3.1.3	Ring Cavity of Q-switched Erbium Doped Fiber Laser	46
<b>CHAPTER 4 RESULTS AND DISCUSSION</b>		<b>48</b>
4.1	Expected Result from Previous Study	49
4.2	Result from my work (MAX phase $Ti_4AlN_3$ )	52
4.3	Result Discussion	60
<b>CHAPTER 5 CONCLUSION AND FUTURE WORKS</b>		<b>65</b>

5.1	Conclusion	66
5.2	Future Works	67
	<b>REFERENCES</b>	<b>69</b>



## LIST OF FIGURES

Figure 2.1: Optical fiber structure .....	21
Figure 2.2: Difference between single-mode and multimode fiber .....	23
Figure 2.3: Typical circuit structure of Er-doped fiber laser .....	25
Figure 2.4: Optical spectrum of Er-doped fiber laser .....	25
Figure 2.5: Non-linear saturated absorption characteristic curve of graphene absorber .....	26
Figure 2.6: Temporal evolution of gain and losses in a passively Q-switched laser .	28
Figure 2.7: Saturable absorber deposited on a D-Shaped fiber .....	30
Figure 2.8: Two methods and a mixture of both are used to exfoliate graphite, increasing the yield and reusing all of the milling products. ....	34
Figure 2.9: Optical properties of MAX-phase <b>Ti<sub>3</sub>AlC<sub>2</sub></b> .....	36
Figure 2.10: EDS spectrum of MAX-phase <b>Ti<sub>3</sub>AlC<sub>2</sub></b> .....	37
Figure 2.11: Raman spectrum of MAX-phase <b>Ti<sub>3</sub>AlC<sub>2</sub></b> .....	37
Figure 2.12: Raman spectrum of MAX-phase <b>Ti<sub>3</sub>AlC<sub>2</sub></b> .....	38
Figure 2.13: nonlinear absorption of MAX-film .....	39
Figure 2.14: nonlinear absorption of MAX-DS .....	40
Figure 3.1: The design of D-shaped fiber polisher.....	43
Figure 3.2: Microscopic image of SMF d-shaped optical fiber (1dB loss) .....	44



Figure 3.3: Microscopic image of SMF d-shaped optical fiber (2dB loss) .....	44
Figure 3.4: MAX solution for integration on d-shaped fiber .....	46
Figure 3.5: Ring cavity of Q-switched Erbium Doped Fiber Laser .....	47
Figure 4.1: The comparison between continuous-wave and Q-switched laser at 126 mW pump power .....	49
Figure 4.2: Oscilloscope trace of pulse train at 126mW pump power.....	50
Figure 4.3: Oscilloscope trace of two pulses within 30 $\mu$ s .....	50
Figure 4.4: The full span of RF spectrum .....	51
Figure 4.5: Repetition rate and pulse width as a function of pump power .....	51
Figure 4.6: Output power, pulse energy, and peak power as a function of pump power .....	52
Figure 4.7: The comparison between continuous-wave and Q-switched laser at 132 mW pump power.....	54
Figure 4.8: Oscilloscope trace of pulse train at 151mW pump power.....	55
Figure 4.9: Oscilloscope trace of two pulses within 20 $\mu$ s .....	56
Figure 4.10: The full span of RF spectrum .....	57
Figure 4.11: The zoomed image at fundamental frequency of RF spectrum .....	58
Figure 4.12: Repetition rate and pulse width as a function of pump power .....	59
Figure 4.13: Output power, pulse energy, and peak power as a function of pump power .....	60

## LIST OF TABLES

Table 4.1: Comparison of performance between saturable absorbers .....	61
--	----



## LIST OF SYMBOLS AND ABBREVIATIONS

For examples:

RF	:	Radio frequency
EDF	:	Erbium doped fiber
2D	:	Two-dimensional
SNR	:	Signal noise ratio
Ti <sub>4</sub> AlN <sub>3</sub>	:	Titanium of four, aluminum of one, and nitrides of three
SA	:	Saturable absorber
SMDFB	:	Single Mode D-shaped Fiber Optic

اونيورسيتي تيكنيكل مليسيا ملاك

UNIVERSITI TEKNIKAL MALAYSIA MELAKA

# CHAPTER 1

## INTRODUCTION



## 1.1 Background of Study

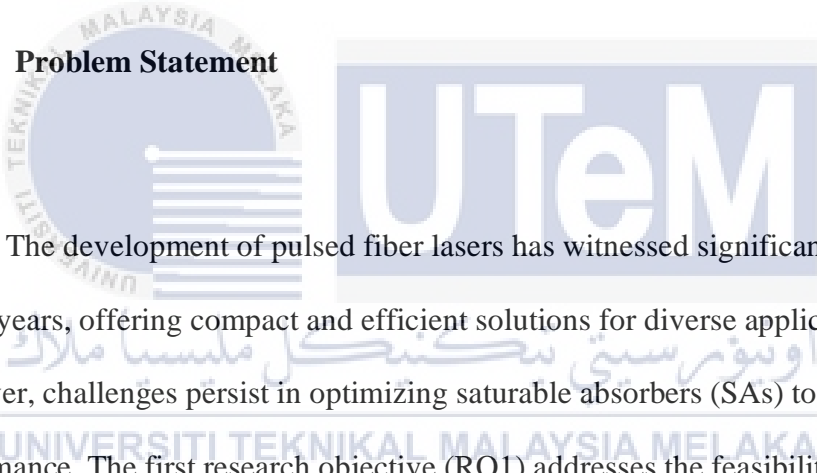
Fiber lasers have emerged as a popular choice for various applications due to their compact size, high power, and excellent beam quality. Pulsed fiber lasers are essential components in diverse technological applications, driven by their compactness, efficiency, and versatility. The heart of these lasers lies in the saturable absorbers (SAs), critical elements that modulate light intensity to produce pulsed laser beams. The quest for optimizing SAs has led researchers to explore unconventional structures and materials. One such avenue is the utilization of D-shaped fiber structures coated with 2D materials, offering a unique geometry for enhanced light absorption and modulation control.

Conventional SAs, while effective, often face limitations in terms of response time and compatibility with intricate fiber optic systems. The D-shaped fiber structure presents a promising alternative, with its flat and curved sides allowing for precise control over light propagation and absorption characteristics. The synergy between this geometric innovation and the incorporation of 2D materials aims to overcome existing SA limitations, offering a pathway to more efficient and responsive pulsed fiber lasers.

In the realm of 2D materials, MAX phase  $Ti_4AlN_3$  emerges as a novel candidate for saturable absorption. Known for its unique combination of metallic and ceramic attributes, MAX phase materials possess remarkable thermal stability, mechanical strength, and electrical conductivity. This project seeks to unravel the untapped potential of MAX phase  $Ti_4AlN_3$  by employing it as a coating material on D-shaped fiber structures.

The significance of this research extends beyond the laboratory, with potential applications in industrial manufacturing, telecommunications, and medical devices. The quest for efficient, cost-effective, and easily manufacturable SAs drives the exploration of these innovative structures. As the pulse of technology quickens, the investigation into D-shaped fiber structures and MAX phase  $Ti_4AlN_3$ -coated fibers promises to shape the future landscape of pulsed fiber lasers, influencing advancements in precision manufacturing, high-speed telecommunications, and medical interventions.

## 1.2 Problem Statement



The development of pulsed fiber lasers has witnessed significant progress in recent years, offering compact and efficient solutions for diverse applications. However, challenges persist in optimizing saturable absorbers (SAs) to enhance laser performance. The first research objective (RO1) addresses the feasibility of utilizing D-shaped fiber structures coated with 2D materials as SAs. Existing SAs often exhibit limitations in terms of response time, efficiency, and compatibility with fiber optic systems. The investigation into D-shaped fiber structures, particularly with the integration of 2D materials, aims to overcome these limitations. However, the specific challenges and potential advantages of this approach require detailed exploration.

Moving to the second research objective (RO2), the focus shifts to analyzing the laser performance of 2D material-coated SM-DFB fibers as SAs in a pulsed fiber laser setup. While advancements have been made in pulse generation using various

SAs, the performance of 2D material-coated fibers, especially in single-mode distributed feedback (SM-DFB) configurations, remains a relatively unexplored territory. Understanding the intricacies of laser performance, including parameters such as pulse width, repetition rate, and output power, is crucial. Furthermore, introducing a novel 2D material, MAX phase  $\text{Ti}_4\text{AlN}_3$ , as a coating material adds a layer of complexity and opportunity to the investigation.

The problem statement, therefore, revolves around the need to address the limitations of existing SAs, explore the potential of D-shaped fibers coated with 2D materials, and comprehensively analyze the laser performance when employing these materials in SM-DFB configurations. The introduction of MAX phase  $\text{Ti}_4\text{AlN}_3$  as a coating material adds an element of novelty, necessitating a thorough investigation to understand its impact on pulsed fiber laser performance. The study aims to contribute insights that can drive advancements in pulsed fiber laser technology and expand the understanding of 2D material-based saturable absorbers.

### 1.3 Objectives

The objectives of this study are:

- i. To study the feasibility of using D-shape fiber structures coated with 2D materials as saturable absorbers for pulsed fiber lasers. (RO1)
- ii. To analyze the laser performance of 2D material-coated SM-DFB fibers as a saturable absorber in a pulsed fiber laser setup. (RO2)

## 1.4 Scope

The project encompasses three key scopes of work to advance the understanding and application of D-shaped fiber structures coated with MAX Phase  $Ti_4AlN_3$  as saturable absorbers. The first scope involves the meticulous fabrication and characterization of D-shaped optical fibers, focusing on optimizing their geometry for efficient light absorption. This step is crucial for ensuring the tailored integration of the saturable absorber into the laser system. Simultaneously, the preparation of MAX Phase  $Ti_4AlN_3$  involves a comprehensive process, including the creation of a solution through the mixing of PVA and  $Ti_4AlN_3$ . This intricate preparation lays the foundation for inducing pulsed fiber laser generation. The final scope is dedicated to the laser performance evaluation of MAX Phase  $Ti_4AlN_3$ . This involves a meticulous analysis of the laser's output, including parameters such as pulse width, repetition rate, output power, and pulse energy. By systematically addressing these three scopes, the project aims to contribute to the optimization and understanding of MAX Phase  $Ti_4AlN_3$ -coated D-shaped fibers, unlocking their potential for advanced applications in pulsed fiber lasers.



## CHAPTER 2

### BACKGROUND STUDY



## 2.1 Fiber lasers

A fiber laser, a type of solid-state laser, operates based on the principle of stimulated emission within an optical fiber. At its core is a gain medium, often a fiber doped with rare-earth ions like erbium or ytterbium. These ions, when energized by an external source (pump), release photons as they return to their lower energy state. This initial photon emission stimulates neighboring ions, initiating a cascade of stimulated emissions, leading to the amplification of light [1].

A resonant cavity, created by reflective elements, provides the necessary feedback to sustain the amplification process and generate a coherent laser beam. The laser output can be modulated by introducing a saturable absorber, which alters its transmission properties based on the input power. This modulation enables the production of short laser pulses, a key feature in applications such as laser surgery or material processing.

Efficient and compact, fiber lasers are widely used in various fields. Their high beam quality and adaptability make them indispensable in telecommunications, where they transmit data over long distances. Additionally, they find applications in materials processing, medical procedures, and scientific research due to their versatility and superior performance characteristics. The unique advantages of fiber lasers position them as crucial components in modern laser technology.

### 2.1.1 Optical fibers

Optical fibers are a type of waveguide that are often composed of glass, have a very long working length, and exhibit great flexibility. Because of its strong mechanical strength against tugging and bending and its potential for low propagation losses (0.2 dB/km at 1550 nm), silica is the most commonly used glass [2]. Figure 2.1 shows the structure of optical fiber.

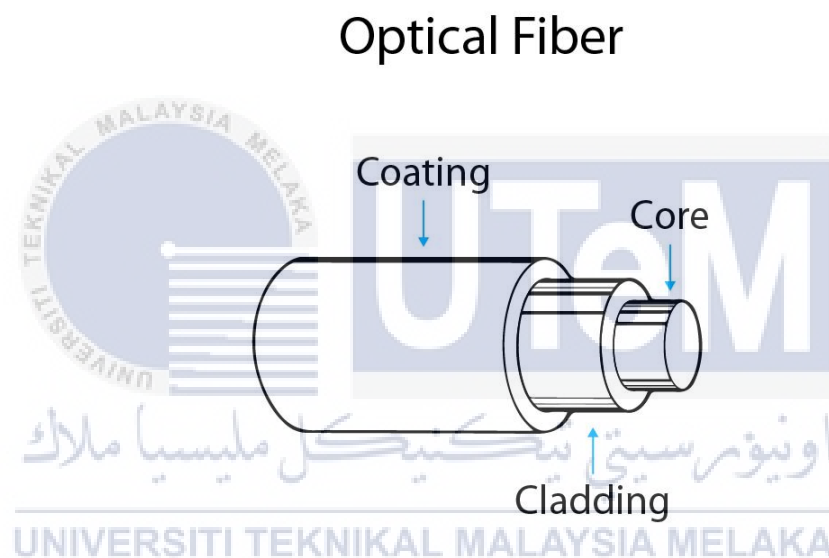


**Figure 2.1: Optical fiber structure**

The components of optical fibers consist of a dielectric core encased in a cladding. Total internal reflection is the process that moves light along the axis. This phenomenon happens when a propagating wave, with respect to the surface normal, impacts a medium barrier at an angle greater than a specified critical angle (the angle of incidence above which the whole internal reflection occurs). The wave cannot pass through and is completely reflected if the index of refraction of the medium the propagated wave contacts is less than that of the media from which it originated.

Having stated that, it is clear that the light's index of refraction needs to be greater than the cladding's in order to contain it within the optical fiber's core.

One may differentiate between single-mode and multi-mode fibers by looking at the propagation modes inside the fibre. The core diameter of multi-mode fibers is significantly greater than the wavelength that they can carry. This length restricts the maximum transmission length because of modal dispersion and permits the propagation of many light modes. A fibre is considered single mode if its core diameter is smaller than roughly 10 times the wavelength of the light it is propagating.

### 2.1.2 Single-mode fiber



An optical fibre type known as single-mode fibre (SMF) is made to only carry one mode of light propagation. Unlike multimode fibers that support multiple light paths (modes), single-mode fibers facilitate the transmission of a single mode of light, providing a higher bandwidth and longer transmission distances. The diameter of core of a single-mode fiber is typically much smaller, around 8 to 10 micrometres, compared to the larger cores of multimode fibers. Figure 2.2 shows difference between single-mode and multimode fiber [3].

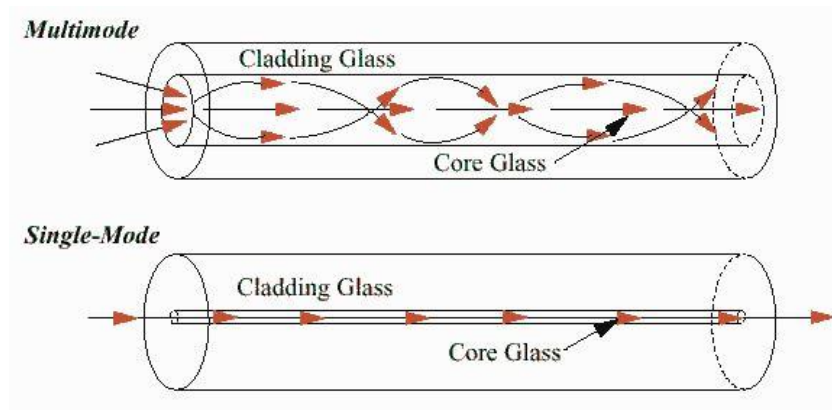


**Figure 2.2: Difference between single-mode and multimode fiber**

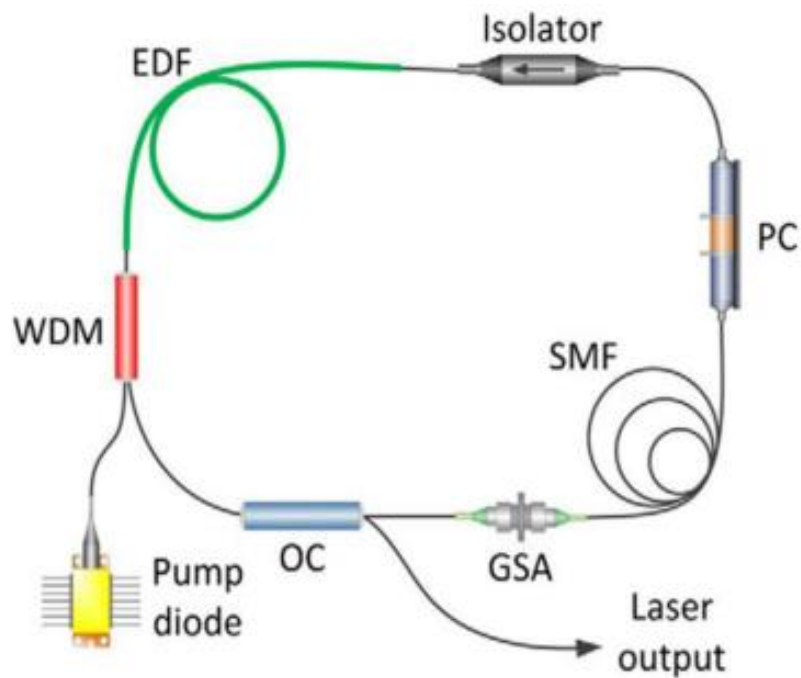
The key characteristic of single-mode fibers is their ability to maintain the integrity of a light signal over longer distances without modal dispersion. Modal dispersion is the phenomenon where different modes of light travel at different speeds, causing distortion in the signal. Single-mode fibers overcome this issue by allowing only one mode of light to propagate, resulting in a more focused and coherent signal.

Single-mode fibers are commonly used in telecommunications for long-distance data transmission, where the minimization of signal loss and distortion is critical. They are also employed in various applications such as fiber optic sensors, high-speed data networks, and laser systems. While single-mode fibers are optimal for long-distance communication, they may have a higher cost and require more precise alignment in the devices using them.

### 2.1.3 Erbium doped fiber lasers

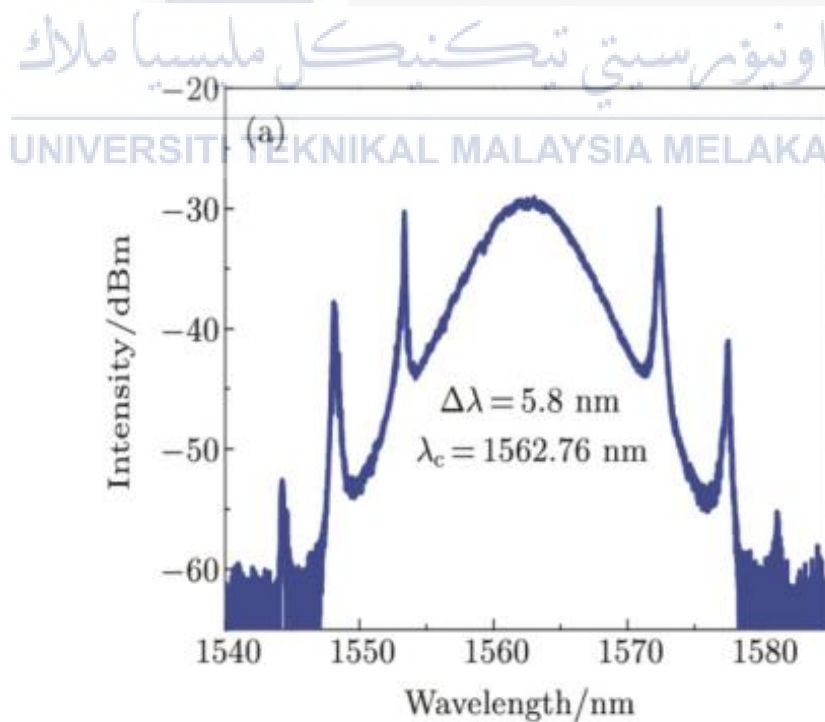
In several kinds of fibre lasers, some material and its oxide-based saturated absorbers are widely utilised. It is crucial to emphasise that Er-doped fibre lasers are extensively utilised due to their affordable price, excellent performance, and straightforward design. The most extensively tested fibre laser in terms of experimentation is the Er-doped fibre laser [4]. Numerous tests have shown graphene's capacity to lock onto a mode in the 3  $\mu\text{m}$  wavelength range. Mode-locked pulses at 2.8  $\mu\text{m}$  with an average output power of 18 mW and a repetition rate of 25.4 MHz have been created by these research, which is equivalent to 0.7nJ of pulse energy [5]. Using a graphene-based SA, Cao et al. demonstrated a wide-band tunable passively Q-switched fibre laser that covered a wavelength range of more than 50.6 nm. The stable Q-switched pulse had a tunable range of 1519.3 nm to 1569.9 nm. [6]. Furthermore, Er-doped lasers produce high repetition rate laser pulses with femtosecond to microsecond durations.

Figure 2.3 depicts the usual circuit structure of an Er-doped fibre laser. It is composed of two FC/APC connectors, a saturable absorber positioned between them, a fibre isolator, a single-mode WDM coupler, an in-line fibre polarization controller, and a long, highly doped erbium fibre [7].



**Figure 2.3: Typical circuit structure of Er-doped fiber laser**

As illustrated in Figure 2.4 [7], the Er-doped fibre laser's output pulse has a centre wavelength of 1.56 $\mu$ m.



**Figure 2.4: Optical spectrum of Er-doped fiber laser**

The fibre material, cavity structure, operating mode, pump type and power, and other parameters all affect the pulse output characteristics of fibre lasers. We must assess the magnitude of its parameters and comprehend their impact on the pulse output of the fibre laser because the modulation depth and saturation also have some influence on the laser's pulse output. A graphene saturable absorber mode-locked erbium-doped fibre laser was proposed by J. SOTOR et al. [8]. With a pulse centre wavelength of 1562 nm, a half-width band of 9 nm, a repetition frequency of 41.9 MHz, and a period of 630 fs, graphene is produced via mechanical exfoliation. They employed a femtosecond laser as the light source in the experiment, and the signal went through a fibre coupler and a variable optical attenuator (VOA) beforehand. Figure 2.5 displays the power dependent gearbox measurement result.

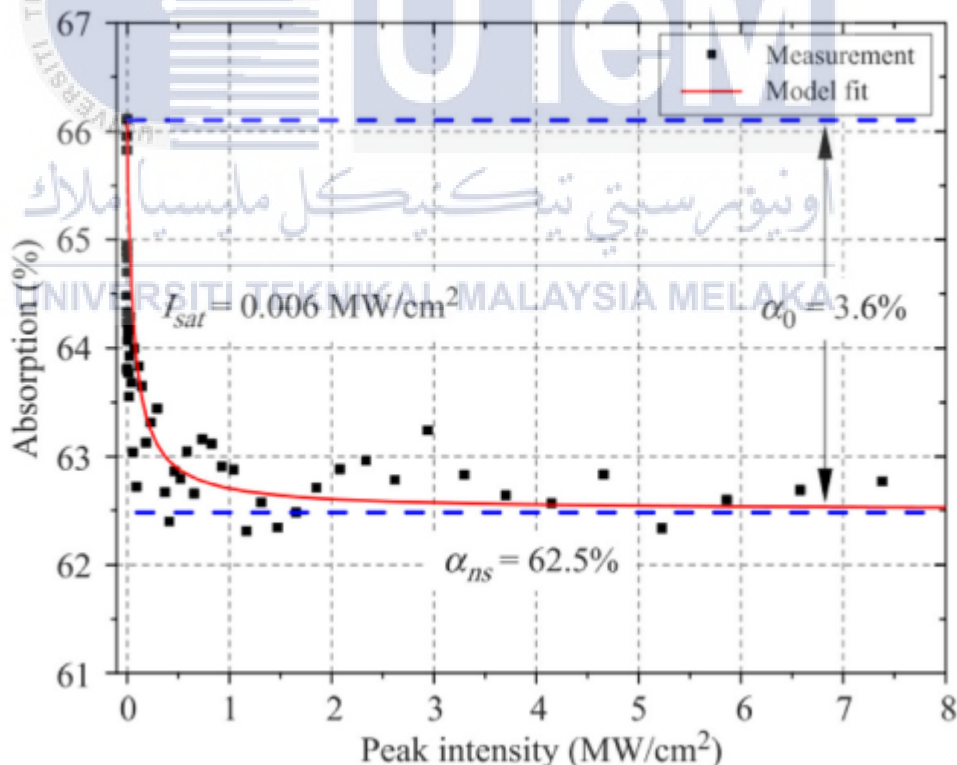


**Figure 2.5: Non-linear saturated absorption characteristic curve of graphene absorber**



The measured data is entered into the following formula to compute the parameters of SA and get the desired outcome.

$$\alpha(I) = \frac{\alpha_0}{1 + \left(\frac{I}{I_{sat}}\right)} + \alpha_{ns}$$

where  $I$  is the light intensity,  $I_{sat}$  is the saturation intensity,  $\alpha_0$  and  $\alpha_{ns}$  are the saturated and non-saturable absorption, respectively, and  $\alpha(I)$  is the absorption coefficient.



#### 2.1.4 Passively Q-switched lasers

For passive Q switching, also known as self Q switching. A saturable absorber is used to automatically control the losses in passive Q switching in Figure 2.6. In this case, the pulse forms as soon as the gain and consequently the energy stored in the gain medium reaches a high enough level. Changes in pump power typically only affect the pulse repetition rate because the energy and duration of the pulses are often fixed which assuming full absorber recovery in between. A brief pulse is released shortly after the laser gain surpasses the resonator losses. When the absorber begins to become saturated, the power increases quickly until the gain reaches the 10% resonator losses threshold [9].

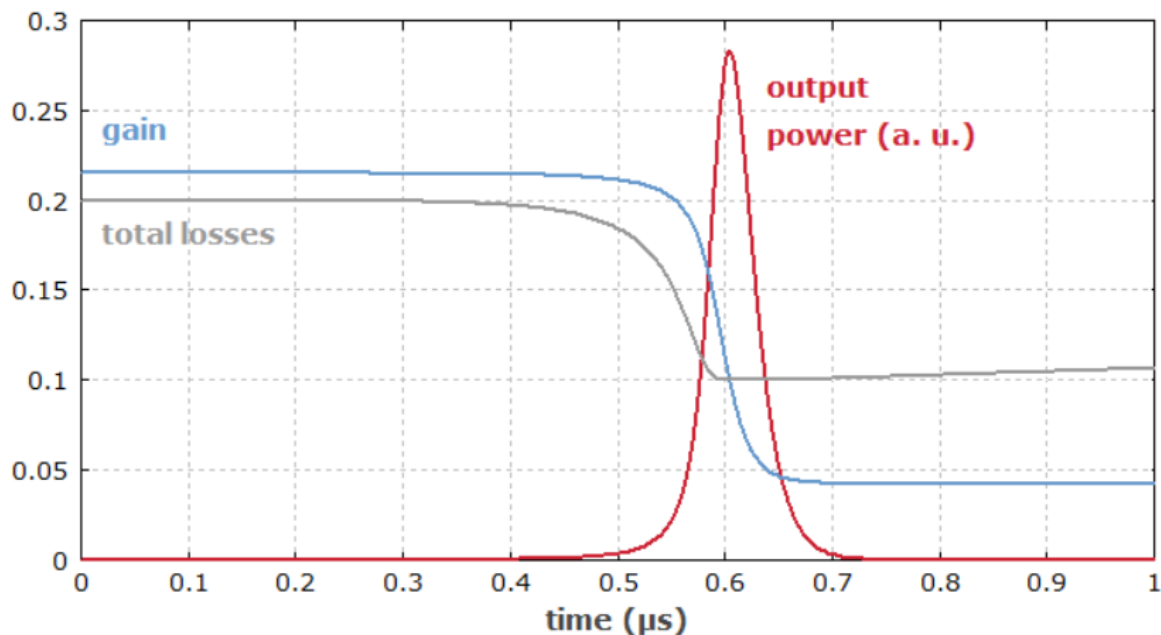


**Figure 2.6: Temporal evolution of gain and losses in a passively Q-switched laser**

Saturable absorber materials such as  $\text{Cr}^{4+}:\text{YAG}$  are widely employed for passive Q switching of  $1\text{-}\mu\text{m}$  YAG lasers.  $\text{Co}^{2+}:\text{MgAl}_2\text{O}_4$ ,  $\text{Co}^{2+}:\text{ZnSe}$ , and other cobalt-doped crystals, as well as glasses doped with PbS quantum dots, are options for  $1.5\text{-}\mu\text{m}$  erbium lasers. Crystals of  $\text{V}^{3+}:\text{YAG}$  are appropriate for the  $1.3\text{-}\mu\text{m}$  range. Semiconductor saturable absorber mirrors are primarily utilized for lower pulse energy and can be utilized at different wavelengths. To prevent further needless energy losses, a saturable absorber's recovery time should preferably be longer than the pulse duration. When the gain recovers, the absorber should be quick enough to avoid premature lasing. The appropriate recovery period is usually found halfway between the pulse duration and the gain medium's upper-state lifespan.

A saturable absorber may, in theory, only absorb a small portion of the energy of the generated pulses; that is, the absorber may not significantly lower the laser's

power efficiency. At the very least, a high efficiency is achievable if (a) the absorber's saturation energy is significantly lower than that of the laser gain medium, (b) the absorber shows very little non-saturable losses, and (c) no other loss channels, like ASE, are involved. Strong focusing may not be able to significantly lower the absorber's saturation energy due to practical constraints like damage thresholds, as real absorbers frequently experience large non-saturable losses. As a result, in actual use, the power efficiency is frequently much decreased.

The resonator round-trip time and the degree of temporal modulation of the net gain determine the pulse duration. The latter is mostly dictated by the saturable absorber's modulation depth. Peak power is increased by both shorter length and greater energy pulses that are typically obtained with a larger modulation depth. The time required to generate the pulse and refill the energy will also increase as a result of the higher energy extraction. Pump power changes frequently have a significant impact on the pulse repetition rate, but they have less of an impact on the pulse's duration, energy, and peak power.

Passive Q switching is simpler and less expensive than active Q switching since it does not require a modulator or associated circuitry, making it appropriate for extremely high pulse repetition rates. The pulse energies are usually lower, though. Furthermore, the pulses cannot be externally triggered (unless an optical pulse from another source is used, which is an uncommon technique). It could also be an issue as the pulse energy and duration are frequently mostly independent of the pump power, which only controls the pulse repetition rate.

## 2.2 D-shaped optical fiber

A polished D-shaped fiber's cladding allows saturable absorber to be deposited in close proximity to the optical fiber's core. Figure 2.7 provides a schematic image of this design for better understanding. By doing this, the evanescent field is made visible, resulting in an interaction with the saturable absorber that shortens pulses by causing saturated absorption [10].

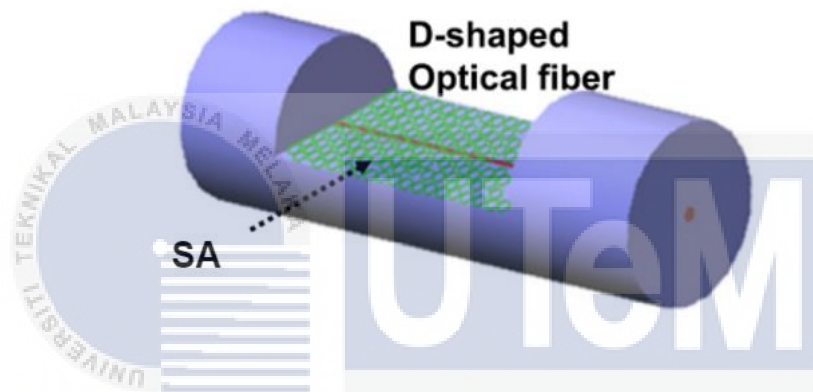


**Figure 2.7: Saturable absorber deposited on a D-Shaped fiber**

The integration of D-shape optical fibers in solid-state lasers represents a vital advancement in laser technology, offering distinct advantages for precise light control and enhanced performance. The unique geometry of D-shaped fibers, characterized by a flat and curved side, enables tailored manipulation of the laser beams characteristics, particularly in the context of solid-state lasers. These fibers serve as efficient saturable absorbers, modulating light intensity and facilitating the generation of short pulses [11].

In solid-state laser systems, the D-shape optical fibers contribute to improved pulse generation, allowing for enhanced control over pulse width and frequency. The

flattened surface of the D-shaped fiber interacts with the evanescent field, influencing the laser's behaviour and enabling diverse applications in areas such as medical procedures, material processing, and telecommunications

Moreover, the integration of D-shaped fibers enhances the overall efficiency of solid-state lasers by optimizing light absorption and modulation. This results in more precise and controlled laser outputs, ensuring superior performance in various industrial and scientific applications. As an integral component in solid-state laser configurations, D-shaped optical fibers underscore their significance in advancing the capabilities and applications of modern laser systems.

Finally, the D-shaped saturation absorber and high output pulse frequency of the fibre laser contribute to its short pulse duration. The laser construction is also simple, affordable, and easy to manufacture. Better optical properties will increase its likelihood of attracting researchers' attention and becoming widely used in a variety of fields in the future.

UNIVERSITI TEKNIKAL MALAYSIA MELAKA

### **2.3 Two-dimensional (2D) materials**

Excellent SA characteristics, such as large modulation depths, large nonlinear optical coefficients, and low saturation intensities, are typically found in two-dimensional (2D) materials [12,13,14]. Because of its zero bandgap and fast carrier relaxation time properties, graphene research is one of the most active areas among them. Many ultra-narrow pulsed fibre lasers at visible, near infrared, and mid-infrared wavelengths have been realised [15]. However, their low damage threshold and

restricted absorption properties in the visible wavelength band prevent them from being used in high-performance systems. Because of their layer-dependent bandgap characteristics and strong nonlinear optical response, layered transition-metal dichalcogenides (TMDs) have also garnered a lot of interest.


In contrast to bulk crystals [13], the 2D materials under discussion are usually layered SA samples. Their broadband absorption properties, high third-order nonlinear magnetization, and thickness-dependent carrier dynamics have demonstrated great potential in pulsed laser systems at visible and near-infrared wavelengths; however, their application at long wavelengths is limited by the bandgap. Furthermore, in the visible wavelength band, they even exhibit superior absorption performance compared to graphene [16].

Liquid dyes are another interesting organic saturable absorber that can be employed for visible wavelength laser pulse production in addition to multilayer materials. But limitations on the laser structure, toxicity, and bleaching vulnerability prevent them from being developed further. Even though low-dimensional SA devices have shown excellent thickness-dependent capabilities in current research at infrared wavelengths, more research on the SA selection mechanism at visible wavelengths is still needed to improve the output performance of visible-wavelength pulsed lasers [17].

Exploring the new 2D material MAX phase represents a frontier in materials science and photonics research [18]. MAX phases are a unique family of layered materials with metallic and ceramic properties, making them lead for various applications. The focus on MAX phase as a saturable absorber (SA) for pulsed fiber lasers introduces a novel dimension to the field. MAX phases, being 2D materials,

hold promise due to their exceptional properties, including high-temperature stability, mechanical robustness, and potential for tailored optical responses. This exploration involves synthesizing and characterizing MAX phase films, understanding their interaction with light, and harnessing these properties for efficient pulse generation in fiber laser systems. The study not only contributes to advancing the understanding of MAX phases but also paves the way for innovative applications in photonics and optoelectronics [19]. The pursuit of this new 2D material reflects the continuous quest for materials with unprecedented functionalities, opening avenues for transformative developments in the realm of optical devices and lasers.

#### 2.4 Saturable absorber



The saturated absorber was made using 2D materials including disulfide, black phosphorus, graphene, and disulfide from transition metals. Examples of methods that have been utilised to create graphene include chemical exfoliation [20], liquid phase exfoliation (LPE) [21], electrochemical approach [22], chemical vapour deposition (CVD) [23], supercritical fluid exfoliation [24], and thermal exfoliation [25]. However, liquid phase exfoliation (LPE) is one of the most important methods for top-down graphene manufacturing. This operation involves the direct exfoliation of graphite to three graphene layers under shear pressures and ultrasonication; it is a simple, low-cost, and environmentally safe procedure without the use of harmful chemicals such strong acids and hydrazine derivatives. A schematic representation of liquid-phase exfoliation can be seen in Figure 2.8.

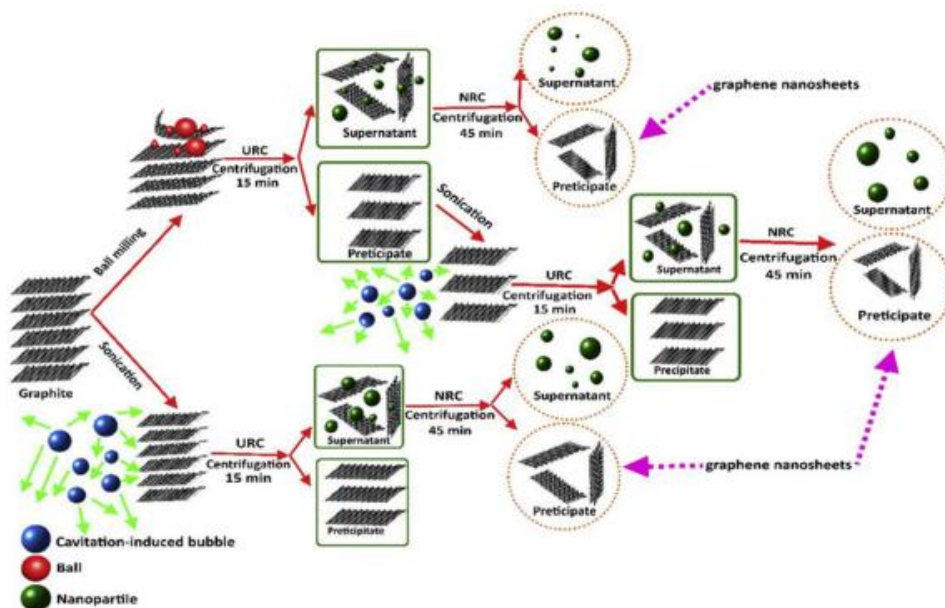


**Figure 2.8: Two methods and a mixture of both are used to exfoliate graphite, increasing the yield and reusing all of the milling products.**

The CVD approach [26] will be the primary focus of this section due to the fact that it is frequently used in many sorts of investigations. To make graphene saturable absorbers, one can utilise chemical methods such scattering graphite sheets in various solvents (dimethyl formamide, polyvinyl alcohol), CVD on Ni/Si substrates [27], or epitaxial growth on SiC substrates. Another successful method is the mechanical exfoliation of graphene from pure graphite, which is based on the highly ordered pyrolytic graphite (HOPG) [28]. The following steps were used to prepare graphene samples using the CVD method: First, monolayer and three-layer graphene thin films were produced on copper foils individually. The copper was then etched using ammonium persulfate. After being thoroughly cleaned in distilled water, the graphene samples were floating on the water. The samples were then dried in nitrogen gas after being fished by quartz substrate [27]. Nowadays, a growing number of studies use Cryogenic liquid stripping in the lab since it is affordable, simple to create, and has reliable performance.



Moreover, the utilization of carbon nanotubes and semiconductor saturable absorber mirrors (SESAMs) in mode-locked lasers has been well-documented [20]. SESAMs, in particular, have been integral in achieving stable and ultrafast pulse generation. The literature emphasizes the significance of SAs in facilitating mode-locking and Q-switching, crucial techniques for generating ultrashort pulses and achieving high peak powers in lasers.

Recent trends showcase a shift towards exploring novel materials like MAX phases [18]. The emergence of MAX phases, as potential SAs introduces a new dimension to the field. The layered structure and unique properties of MAX phases offer exciting possibilities for tailoring their interaction with light, paving the way for advanced applications in pulsed fiber lasers [19].

#### 2.4.1 MAX phase as saturable absorber

The standard formula for the MAX phases, which is a layered, hexagonal carbides and nitrides that make up the is  $M_{n+1}AX_n$ , (MAX), where n ranges from 1 to 4. In this formula, M represents an early transition metal, A is an element from the A-group (usually IIIA and IVA, or groups 13 and 14), and X can be either carbon or nitrogen. The A-group element's single planar layers are sandwiched between edge-sharing, deformed  $XM_6$  octahedra in the layered structure. Excellent oxidation resistance, a high modulus of elasticity, low density, and a high melting temperature are some of the unique physical properties of the MAX phases that make them a good material for a variety of industrial applications [29]. In contrast to other 2D materials, it may be easily used as SA without requiring a time-consuming preparatory phase. Additionally, a promising saturable absorption is seen in the bulky MAX phase in the

broad near-infrared spectrum bandwidth. It can effectively produce a pulsed laser in the erbium, ytterbium, and thulium-doped fibre laser cavities and has a modulation depth of 2–60% in the 1.55  $\mu\text{m}$  [30]. In comparison to other 2D materials that have been thoroughly studied, such as  $\text{Ti}_3\text{C}_2\text{T}_x$  [31],  $\text{Ti}_3\text{CNT}_x$  [32],  $\text{WSe}_2$  [33],  $\text{WS}_2$  [34],  $\text{MoS}_2$  [35], and  $\text{Bi}_2\text{Te}_3$  [36], the obtained saturable absorption was higher. Given this, we looked at the possibility of the MAX phases acting as a SA in an EDFL cavity.

In a study [37], a variable-pressure scanning electron microscopy (VPSEM) image of the produced  $\text{Ti}_3\text{AlC}_2$  MAX phase is shown in Figure 2.9. The particle size distribution was found to be around 10  $\mu\text{m}$ . In order to verify the MAX solution's elemental composition, energy dispersive x-ray spectroscopy (EDS) was employed.

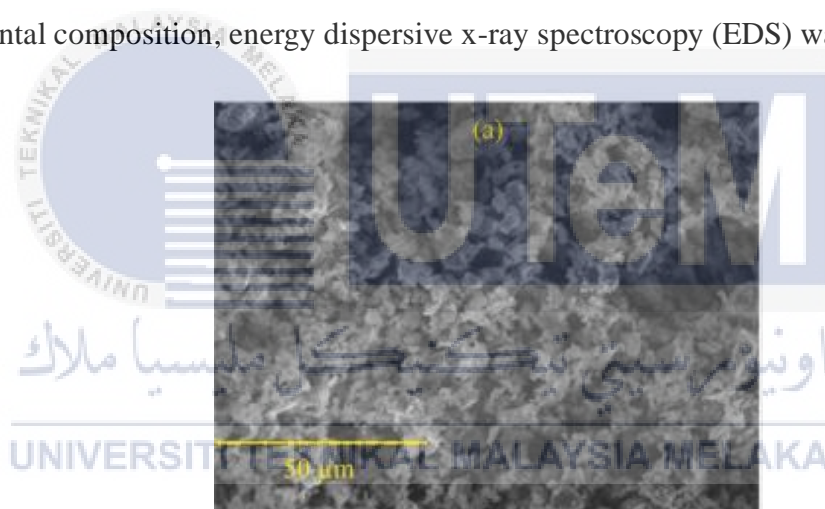


**Figure 2.9: Optical properties of MAX-phase  $\text{Ti}_3\text{AlC}_2$**

The resulting spectrum with 73.2 weight percent titanium (Ti), 10.5 weight percent aluminum (Al), 9.3 weight percent carbon (C), and 7.0 weight percent oxygen (O) is shown in Figure 2.10.

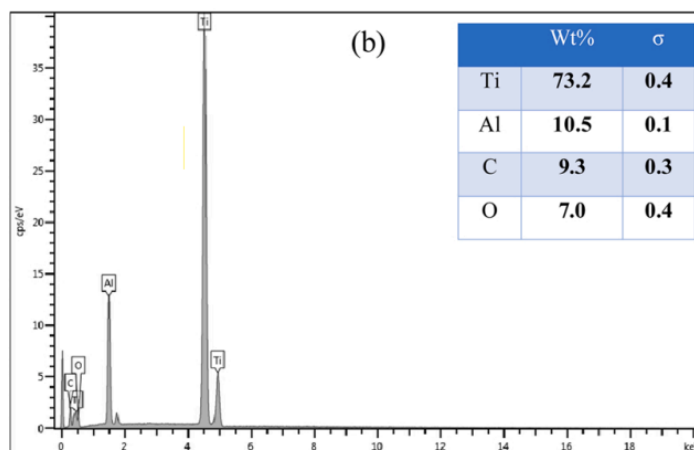


**Figure 2.10: EDS spectrum of MAX-phase  $Ti_3AlC_2$**

For Raman Spectroscopy, a 532 nm frequency doubled YAG laser stimulated on top of the  $Ti_3AlC_2$  solution. As shown in Figure 2.11, the vibrational modes of the as-prepared SA indicated 4 characteristic peaks of MAX-phase  $Ti_3AlC_2$  composition. On the recorded spectra, the Raman shift was noticeable at wavenumbers of 171  $cm^{-1}$  ( $E_g$ ), 407  $cm^{-1}$  ( $E_{2g}$ ), 517  $cm^{-1}$  ( $E_{1g}$ ), and 638  $cm^{-1}$  ( $A_{1g}$ ). Disordered carbon is represented by two peaks that almost completely disappear at wavenumbers of 1360  $cm^{-1}$  ( $A_{1g}$ ) and 1605  $cm^{-1}$  ( $E_{2g}$ ) in the  $Ti_3AlC_2$  component.

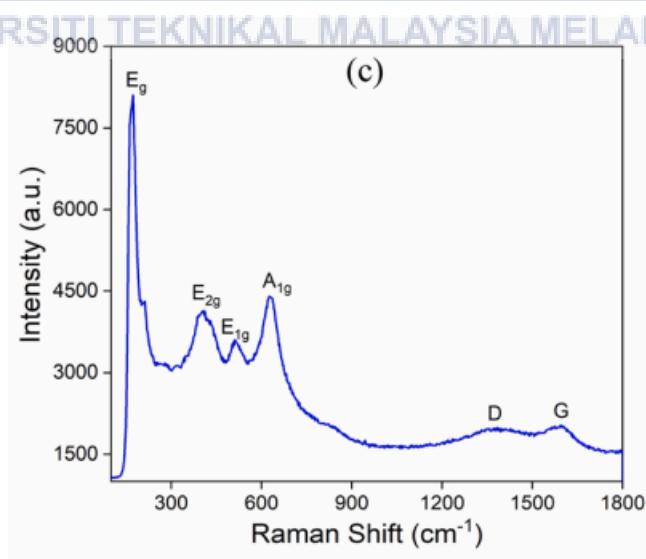


**Figure 2.11: Raman spectrum of MAX-phase  $Ti_3AlC_2$**

The linear absorption properties of MAX-film and MAX-DS were then examined. At the operating wavelength of 1560 nm, MAX-DS showed 5.5 dB absorption, as shown in Figure 2.12. observed a nearly smooth absorption line for MAX-film at the same wavelength, with an absorption of 3.4 dB. It has been confirmed that both SA devices exhibit wideband absorption in the 1.55- $\mu\text{m}$  area, which spans from 1250 to 1560 nm.

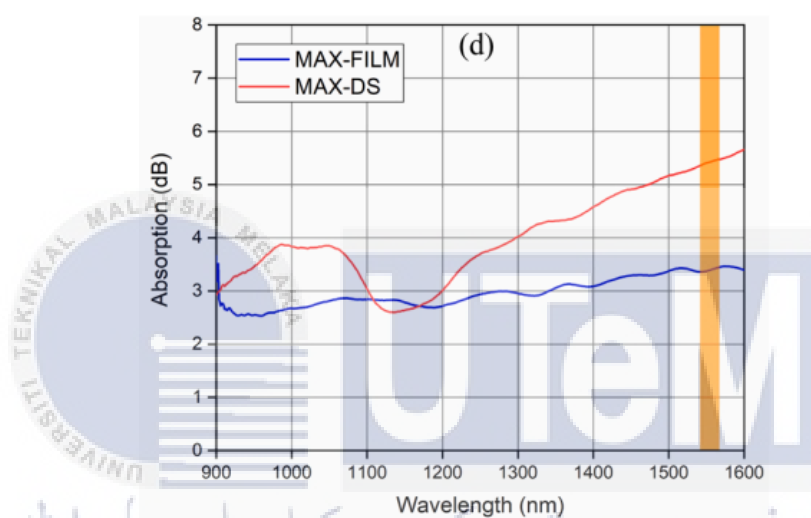


**Figure 2.12: Raman spectrum of MAX-phase  $Ti_3AlC_2$**   
UNIVERSITI TEKNIKAL MALAYSIA MELAKA

Used a twin-balanced detector technique to look at MAX-film and MAX-DS's nonlinear saturable absorption. For the measurement, we used a steady mode-locked source with a repetition rate of 1.885 MHz, a pulse width of 3.62 ps, and a center wavelength of 1557.7 nm. An erbium-doped fibre amplifier (EDFA) that doubles as an optical attenuator and a laser intensity modulator can be used to increase the peak. Divide the pulse so that the signal is distributed in two directions using a 3 dB coupler. Half of the light travels over a naked single-mode optical fibre (SMF-28) while the other half strikes the SA. The data were fitted using Equation, where  $\alpha(I)$  represents a total intensity-dependent absorption coefficient,  $\alpha_0$  a linear absorption coefficient,

$I_{sat}$  a saturation intensity, and  $\alpha_{ns}$  as non-saturable absorption. Plotting the nonlinear absorption spectra of both SAs, as shown in Figure 2.13 and 2.14, indicates the identical modulation depth value of 2%. MAX-film shows a saturable intensity of 1.69 MW/cm<sup>2</sup> and a non-saturable absorption of 58.2%. On the other hand, MAX-DS showed a somewhat modest non-saturable absorption with a saturable intensity of 2.68 MW/cm<sup>2</sup>.

$$\alpha(I) = \frac{\alpha_0}{1 + \left(\frac{I}{I_{sat}}\right)} + \alpha_{ns}$$

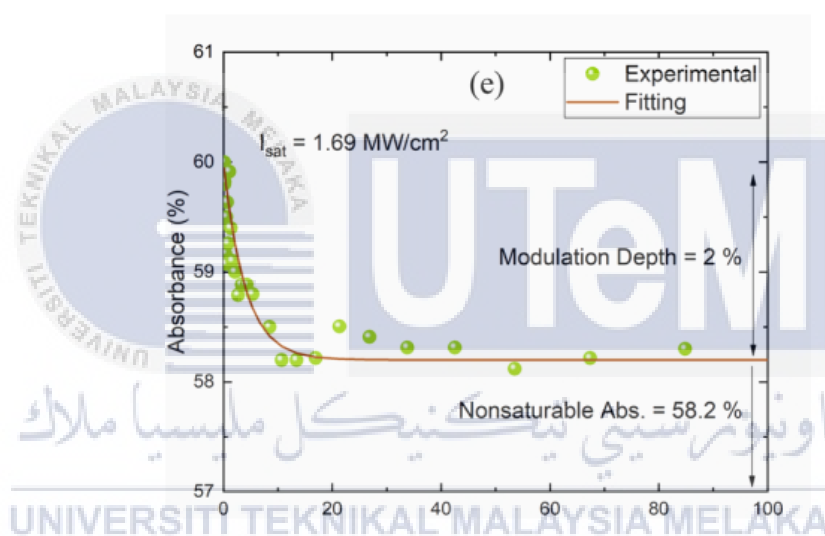


**Figure 2.13: nonlinear absorption of MAX-film**

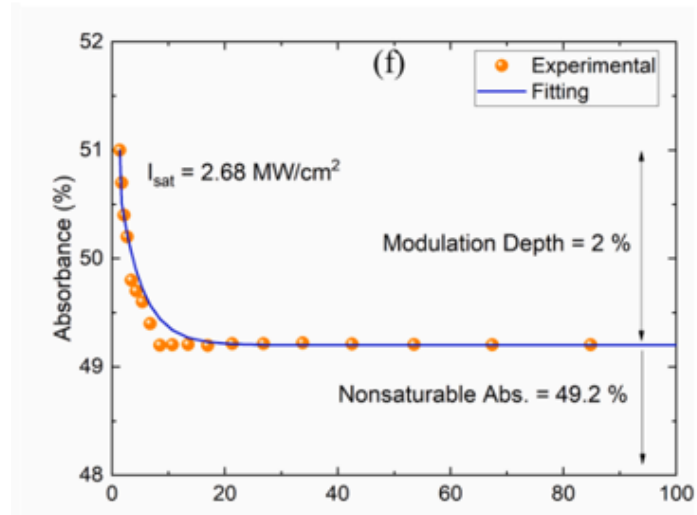


Figure 2.14: nonlinear absorption of MAX-DS



## CHAPTER 3

### METHODOLOGY



### 3.1 Fabrication of Saturable Absorber

Saturable absorber fabrication involves two essential processes: D-shaped fiber fabrication and the creation of the MAX phase solution. In D-shaped fiber preparation, a polishing machine is employed to remove one side of the optical fiber. Material fabrication entails two distinct steps: the preparation of a PVA solution as a base material and the mixing of the PVA solution with MAX phase powder. Following the completion of each preparation, the MAX phase solution is deposited onto the D-shaped region to initiate the pulse fiber laser.

#### 3.1.1 Fabrication of D-shaped Fiber Optic

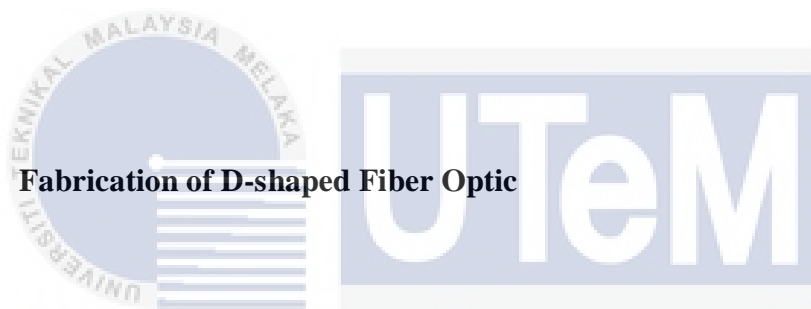
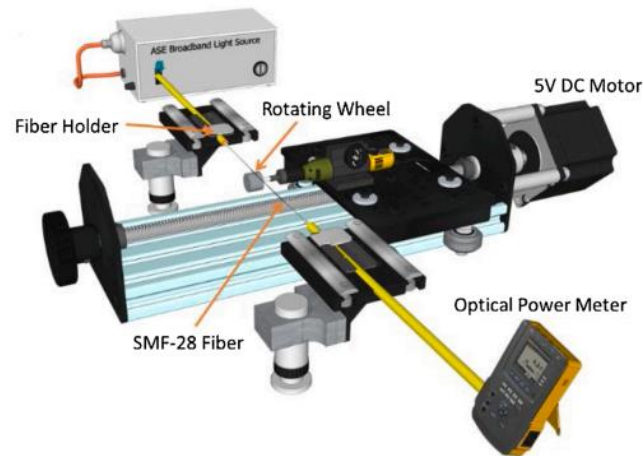


Figure 3.1 shows the D-shaped fibre polisher that we designed. The proposed experimental setup consists of an amplified stimulated emission (ASE) broadband light source, two fibre holders, an adjustable stage, a mechanical wheel with sandpaper, a 5-volt (5 V) DC motor, and an optical power meter. Splicing two fiber-ferrules together with a single-mode optical fibre (SMF-28) is the first step in the experimental process. We took off about 5 mm of fibre covering to reveal SMF-28's cladding. Using two fibre holders as a clamper, the SMF-28 was set up and linked to the ASE source. The other end of the device was placed onto an optical power meter. After correctly adjusting the mechanical wheel with sandpaper so that it touches the uncoated zone of SMF-28, the 5 V DC motor was turned on. It is ensured that the right



amount of cladding was removed by real-time measurement. Our 15-minute D-shaped fibre production technology guarantees a quick SA preparation process.



**Figure 3.1: The design of D-shaped fiber polisher**

### 3.1.1.1 Insertion Loss of D-shaped Fiber

The insertion loss of single mode D-shaped fiber during polishing refers to the reduction in optical signal power caused by the removal of material during the polishing process. The suitable insertion loss for D-shaped fiber is important so that the absorption of saturable absorber will be more efficient during the integration. A few insertions loss of single mode D-shaped fiber have been attempted and compared so the absorption of the saturable absorber is ensured. Microscopy in the lab is used to generate a microscopic image of a 0.5mm fiber optic. Figure 3.2 shows the microscopic image of SMF d-shaped optical fiber of 1dB loss, which the fiber optic is polished from 0.13mm to 0.08mm.

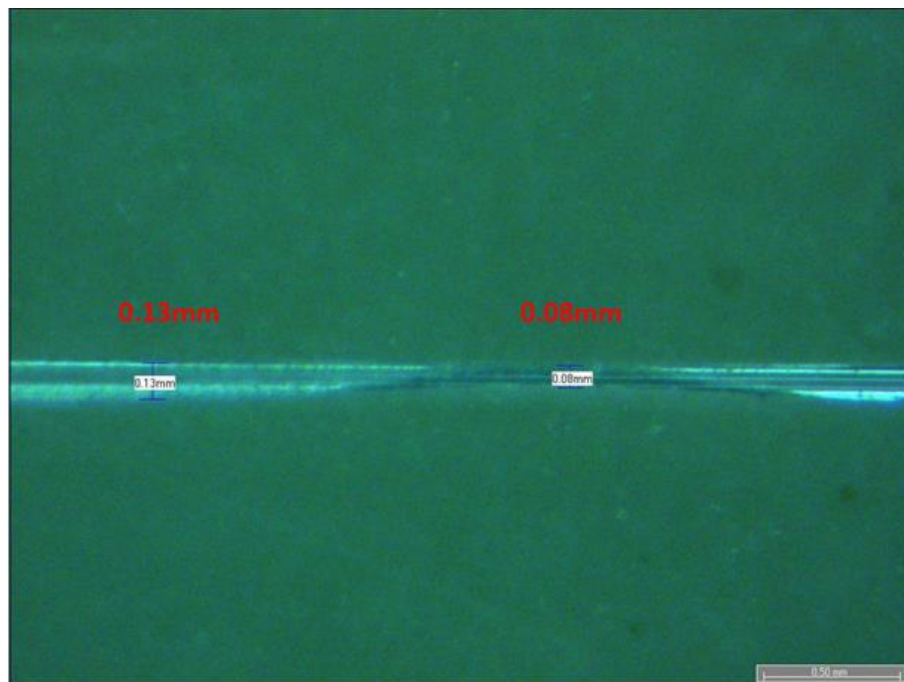


**Figure 3.2: Microscopic image of SMF d-shaped optical fiber (1dB loss)**

Figure 3.3 shows the microscopic image of SMF d-shaped optical fiber of 2dB loss, which the fiber optic is polished from 0.13mm to 0.07mm.

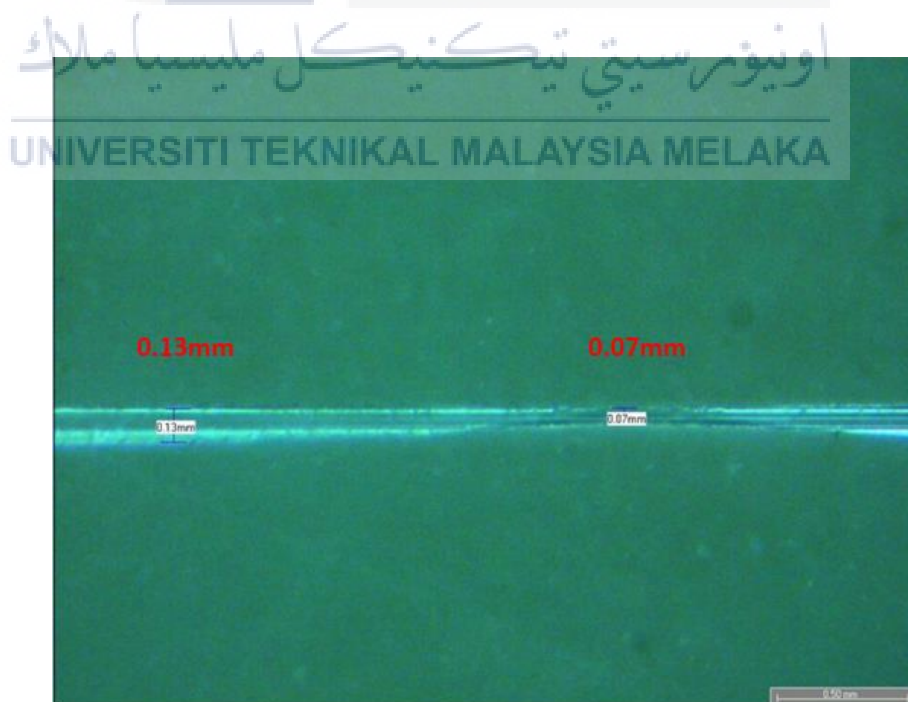


**Figure 3.3: Microscopic image of SMF d-shaped optical fiber (2dB loss)**

While 3db loss for SMF d-shaped optical fiber is failed because of the fragile fiber optic so that is not considered. Then, the absorption of saturable absorber is compared between 1dB loss and 2dB loss by using integration on the D-shaped fiber and the performance of pulsed fiber laser is analyzed. After that, the 2dB loss of SMF d-shaped optical fiber is chosen because the absorption efficiency is better than the 1dB loss of SMF d-shaped optical fiber.

### 3.1.2 Preparation of MAX phase $Ti_4AlN_3$

Firstly, we use the PVA solution and  $Ti_4AlN_3$  powder to synthesis the MAX solution. Initially, we mixed 1 gram of PVA powder with 120 mL of deionized (DI) water to create the PVA solution. Using a 300-rpm rotating speed, we stirred the mixture on a hot plate for 24 hours at 90 °C.

After that, to prepare the MAX Phase solution, a meticulous step-by-step process was followed. First, a well-balanced mixture was created by combining 30 mL of polyvinyl alcohol (PVA) with 60 mg of  $Ti_4AlN_3$  in a precise 1:2 ratio. The mixture underwent thorough stirring for 24 hours at room temperature, ensuring the homogeneity of the solution. Subsequently, to enhance the dispersion and eliminate any potential cohesions, the solution underwent a 45-minute ultrasonic bath treatment. This ultrasonic bath step was repeated three times, underscoring the commitment to achieving a uniformly dispersed and stable MAX Phase solution. Each step in this meticulous preparation process was undertaken with precision to ensure the quality and reliability of the MAX Phase solution for subsequent applications in the project.

Later, the remaining MAX solution was placed in a tube and readily used as a SA for D-shaped fiber. Figure 3.4 shows the MAX solution for integration on d-shaped fiber.

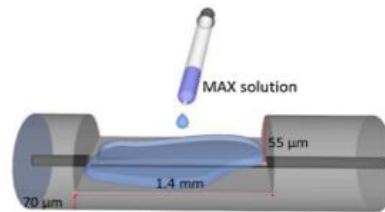


**Figure 3.4: MAX solution for integration on d-shaped fiber**

### 3.1.3 Ring Cavity of Q-switched Erbium Doped Fiber Laser

Figure 3.5 depicts the arrangement of the proposed Q-switched Erbium-Doped Fiber Laser (EDFL) employing a ring cavity design with Saturable Absorber (SA) implementation techniques. The EDFL cavity comprises a 2.4 m-long Erbium-Doped Fiber (EDF) serving as the gain medium, pumped by a butterfly-mounted 980 nm laser diode through a 980/1550 wavelength division multiplexer (WDM). The optical setup also includes an optical isolator at 1550 nm (OPLINK) to ensure unidirectional light propagation within the cavity, an 80/20 optical coupler (JDSU E-TEK 1550 nm SMF-28) splitting light into two paths (80% circulating in the cavity, 20% connected to measuring instruments).

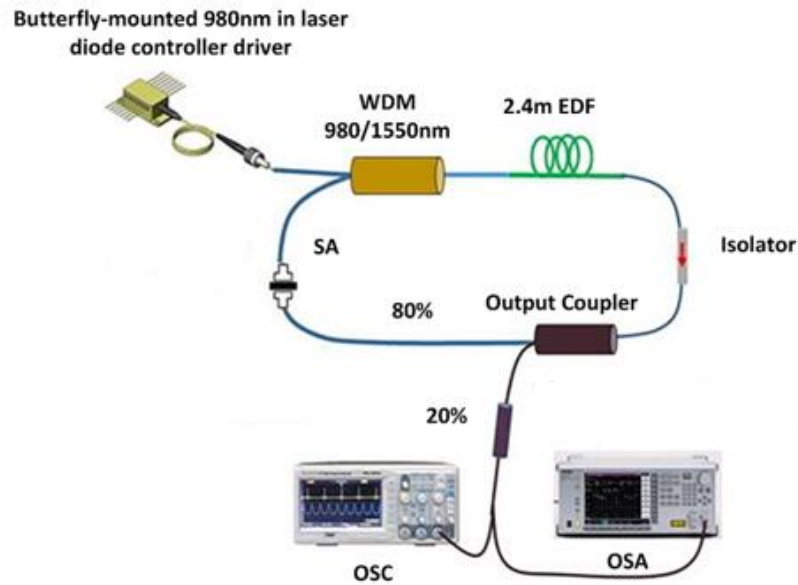


**Figure 3.5: Ring cavity of Q-switched Erbium Doped Fiber Laser**

To minimize losses, no polarization controller (PC) was used, and all fiber connections in the cavity were fusion spliced. In this experiment, the MAX-DS was directly spliced into the EDFL. Using a micropipette, the MAX solution was gradually applied to the polished side of the D-shaped fibre until an oscilloscope showed a stable pulse train. Using an optical power meter (PM100D Thorlabs) and an optical spectrum analyzer (Anritsu MS9710C: 7001750 nm), the spectral and intensity-dependent features of the Q-switched EDFL were studied. A radio-frequency spectrum analyzer (RFSA-Anritsu MS2683A 9 kHz-7.8 GHz) and a 350 MHz 5GS/s digital oscilloscope (GWINSTEK: GDS-3352) were used to capture the temporal properties of the produced pulses. They were coupled by a 1.2 GHz InGaAs photodetector (Thorlabs: DET01CGC). For MAX phase D-shaped fiber, the overall cavity length was 14.6 m.

## CHAPTER 4

### RESULTS AND DISCUSSION



#### 4.1 Expected Result from Previous Study

This is a study result for MAX phase as saturable absorber coated on D-shaped optical fiber. As shown in Figure 4.1, the continuous-wave laser was recorded at a wavelength of 1559.3 nm. When the pulse laser was induced, the MAX phase solution was applied to a D-shaped area. The pulsed laser was visible under a digital oscilloscope at a pump power of 90 mW; the pump power was then increased to 126 mW which is the maximum power for the experiment. The Q-switched pulsed laser first appeared at 1558.2 nm, which is slightly left of the continuous-wave wavelength, according to the optical spectrum analyzer.

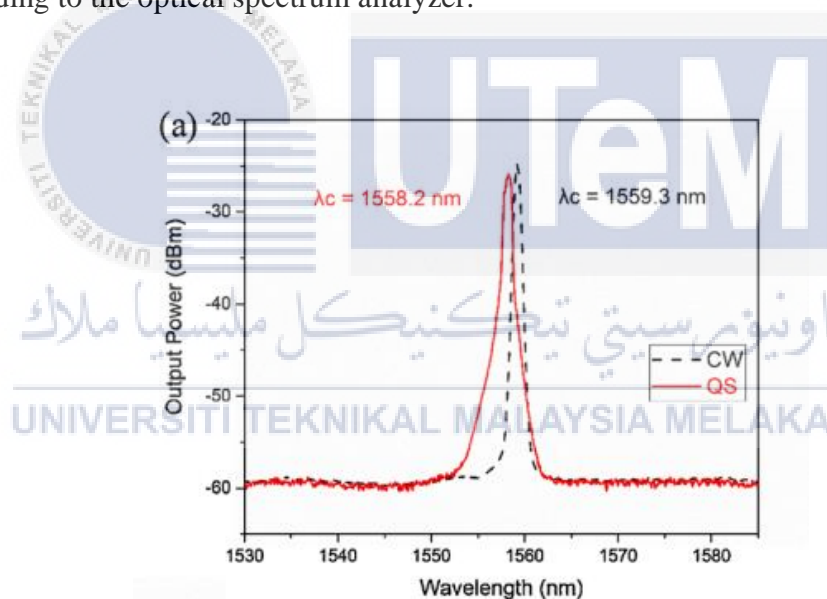


**Figure 4.1: The comparison between continuous-wave and Q-switched laser at 126 mW pump power**

The temporal properties of the produced pulses were then examined using a digital oscilloscope. The oscilloscope trace with a series pulse over an 800  $\mu$ s interval is displayed in Figure 4.2.

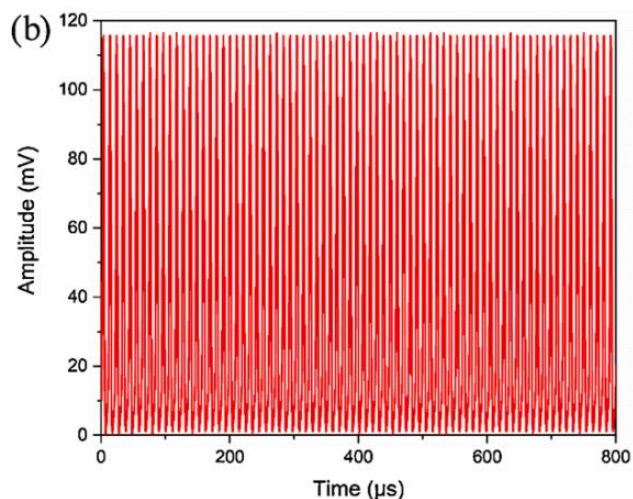


**Figure 4.2: Oscilloscope trace of pulse train at 126mW pump power**

As seen in Figure 4.3, the pulses were displayed in an inset image of two pulse envelopes at maximum pump power, with a pulse width of  $2.933 \mu\text{s}$  and a pulse period of  $10.4 \mu\text{s}$ .

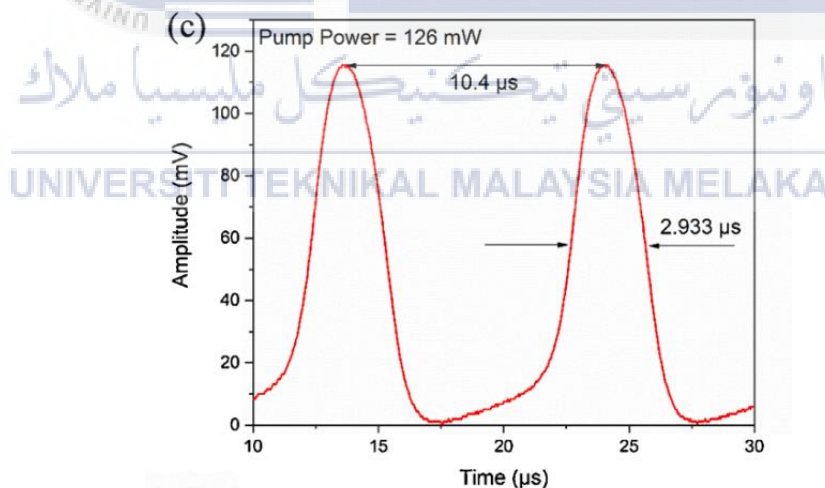


**Figure 4.3: Oscilloscope trace of two pulses within  $30\mu\text{s}$**

The RF spectrum was recorded at the maximum pump power of 126 mW, as shown in Figure 4.4. The harmonic peak that decreased from high to low output power indicates that the Q-switched pulse laser generation in the EDFL ring cavity was



steady, and the signal-to-noise ratio (SNR) was measured at 70 dB. The first peak was identified as the 96.15 kHz fundamental frequency, or repetition rate, which corresponds to the pulsed wave that was observed using a digital oscilloscope.

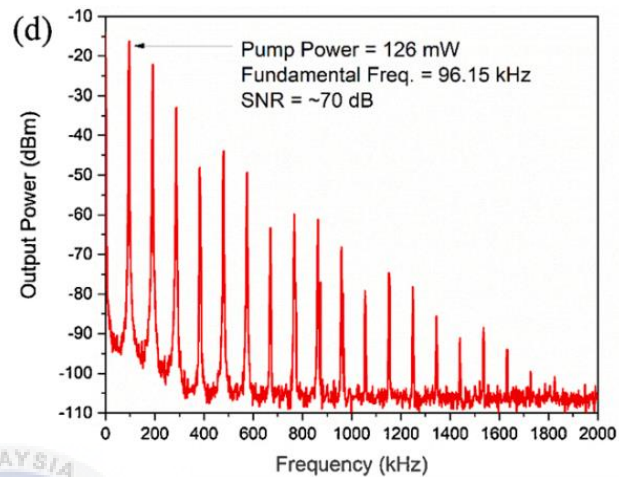


**Figure 4.4: The full span of RF spectrum**

The plotted graph of repetition rate vs pulse width as a function of pump power is displayed in Figure 4.5. When the pump power was raised, the repetition rate inclined between 79.62 and 96.15 kHz. The pulse width decreased from 4.1 to 2.93  $\mu\text{s}$  while the pump power increased to 62–126 mW.

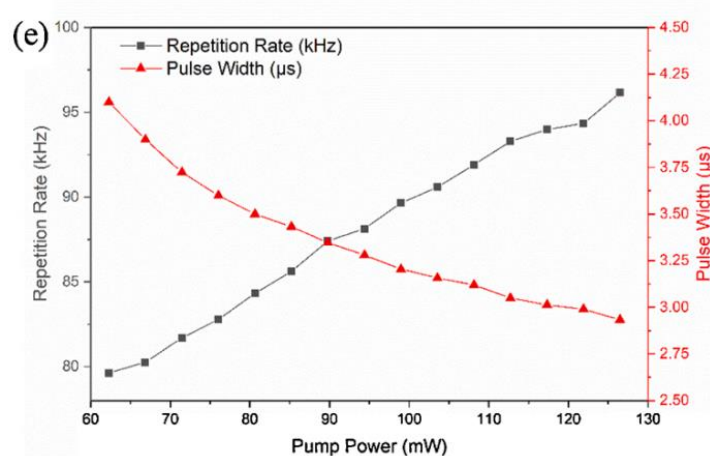


**Figure 4.5: Repetition rate and pulse width as a function of pump power**

The output power, pulse energy, and peak power rose linearly with the pump power, as shown in Figure 4.6. A range of 7.5 to 14.6 mW was measured for the output power. Peak power and pulse energy were 51.77 mW and 151.8 nJ, respectively, at their maximums. Additionally, a measurement of 11% slope efficiency between output power and pump power was made.

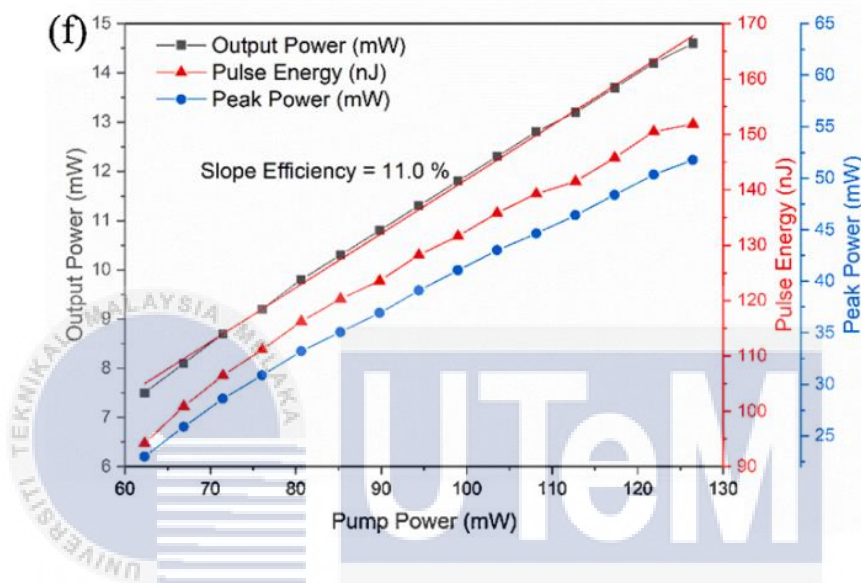


Figure 4.6: Output power, pulse energy, and peak power as a function of pump power

#### 4.2 Result from my work (MAX phase $\text{Ti}_4\text{AlN}_3$ )

For this project, the comprehensive analysis of various parameters is significant in understanding the performance of pulsed fiber lasers. The pulsed laser spectrum provides insights into the distribution of optical power across different wavelengths, crucial for applications such as material processing and telecommunications. The oscilloscope trace of the pulse train unveils the temporal

characteristics, depicting the arrangement and duration of individual pulses. The radio-frequency (RF) spectrum further scrutinizes the signal-to-noise ratio (SNR) and the fundamental frequency, offering a detailed view of the pulse train's stability. Additionally, examining the relationship between repetition rate, pulse width, output power, pulse energy, and peak power concerning pump power sheds light on the laser's efficiency and scalability. This multifaceted exploration of parameters contributes to a nuanced understanding of the pulsed fiber laser's behaviour and its potential applications.

Pump power is the optical power supplied to the gain medium of a laser system to initiate the process of stimulated emission. The pump power is a crucial parameter as it determines the efficiency and performance of the laser system. Higher pump power can lead to increased gain in the gain medium, resulting in higher output power. However, there is an optimal pump power range for efficient laser operation, and exceeding this range may lead to undesired effects like thermal issues or damage to the gain medium. In this project, the maximum pump power is set to 151mW as increased of it will be harmful for the components and equipment itself.

The Q-switched pulsed laser spectrum at 151 mW of pump power is contrasted with the continuous-wave lasing as seen in Figure 4.7. In light of observation, the wavelength of Q-switched was shifted to the left as much as 28.2 nm due to the presence of Ti4AlN3. The central wavelength of Q-switched pulsed laser at 1533.6 nm and a peak intensity of -2.9 dBm. While the central spectrum for continuous-wave lasing was at 1561.8 nm with a peak intensity of 2.4 dBm. It shows that there is an insertion loss occurs when the D-shaped fiber integrated with the EDFL ring cavity.

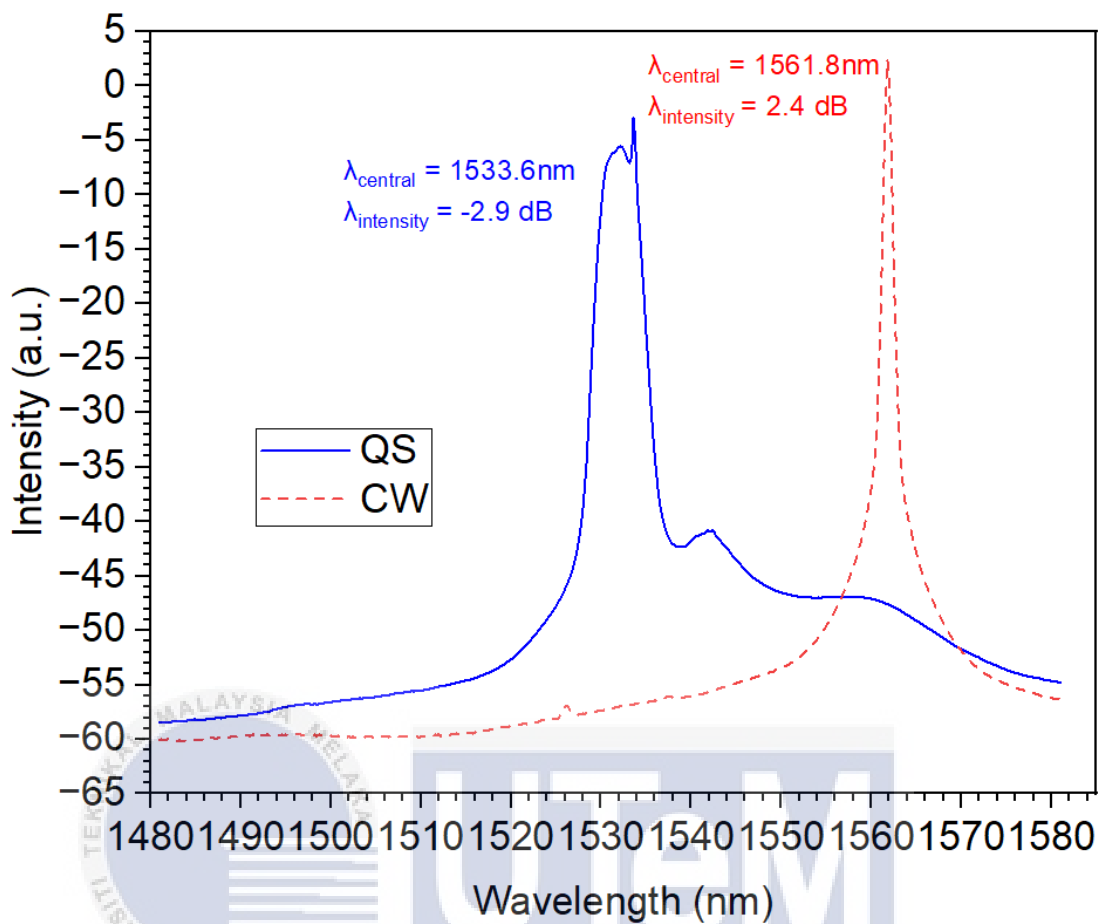


**Figure 4.7: The comparison between continuous-wave and Q-switched laser at 132 mW pump power**

In Figure 4.8, it illustrates the pulse train of Q-switched pulse laser at maximum pump power of 151 mW which indicates a stable pulse. When the pump power is increased exceed 151 mW, the pulse train fades slowly and becomes continuous-wave lasing.

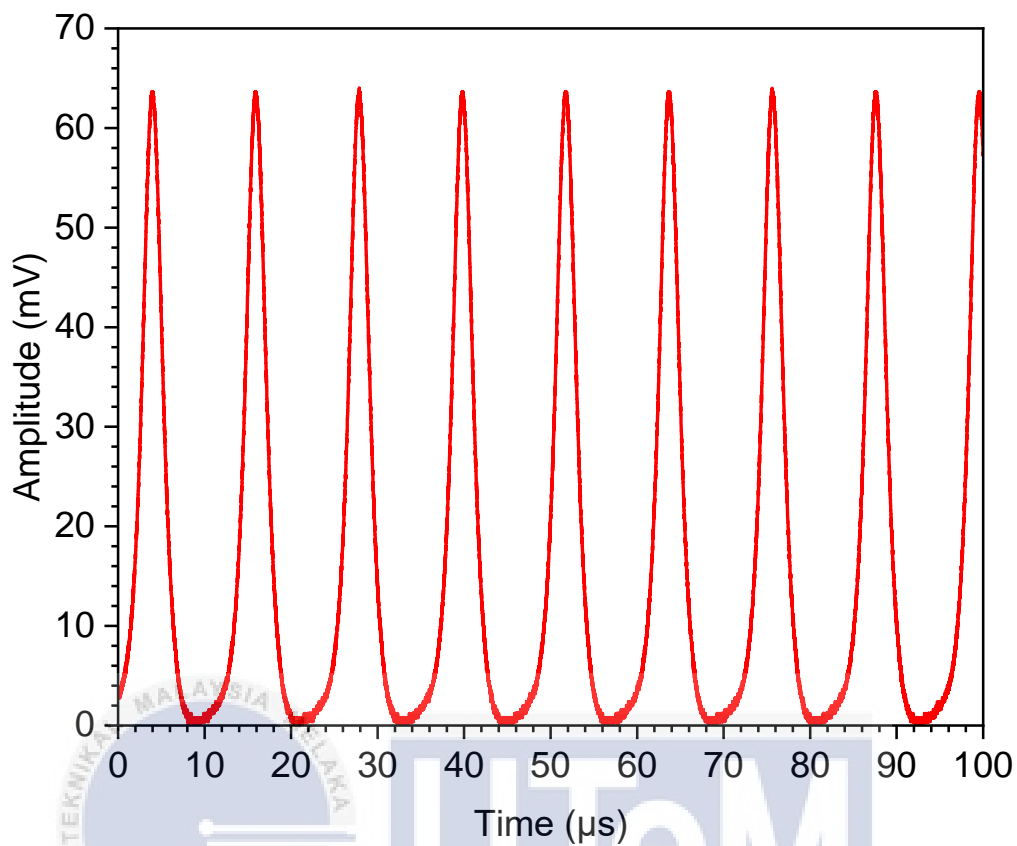


**Figure 4.8: Oscilloscope trace of pulse train at 151mW pump power**

The pulse width was recorded in digital oscilloscope, it shows that the minimum pulse width was achieved which is 2.62  $\mu\text{s}$  while the pulse period between two peak of pulses is 11.94  $\mu\text{s}$  as shown in Figure 4.9.

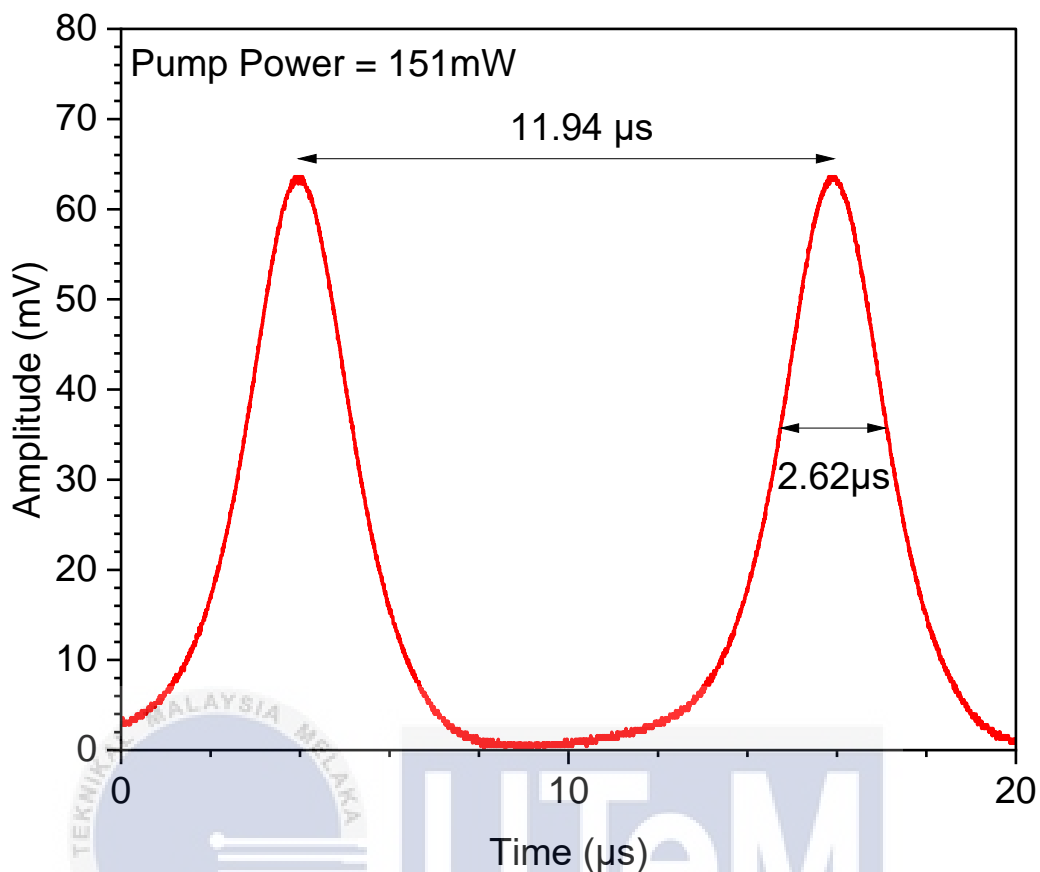


**Figure 4.9: Oscilloscope trace of two pulses within 20 $\mu\text{s}$**

The repetition rate was captured during using oscilloscope at maximum pump power which is 83.7 kHz. Figure 4.10 shows the RF spectrum pulsed laser at pump power of 151 mW, The first peak of fundamental frequency indicates 83.7 kHz which is equivalent to the repetition rate that recorded by using digital oscilloscope.

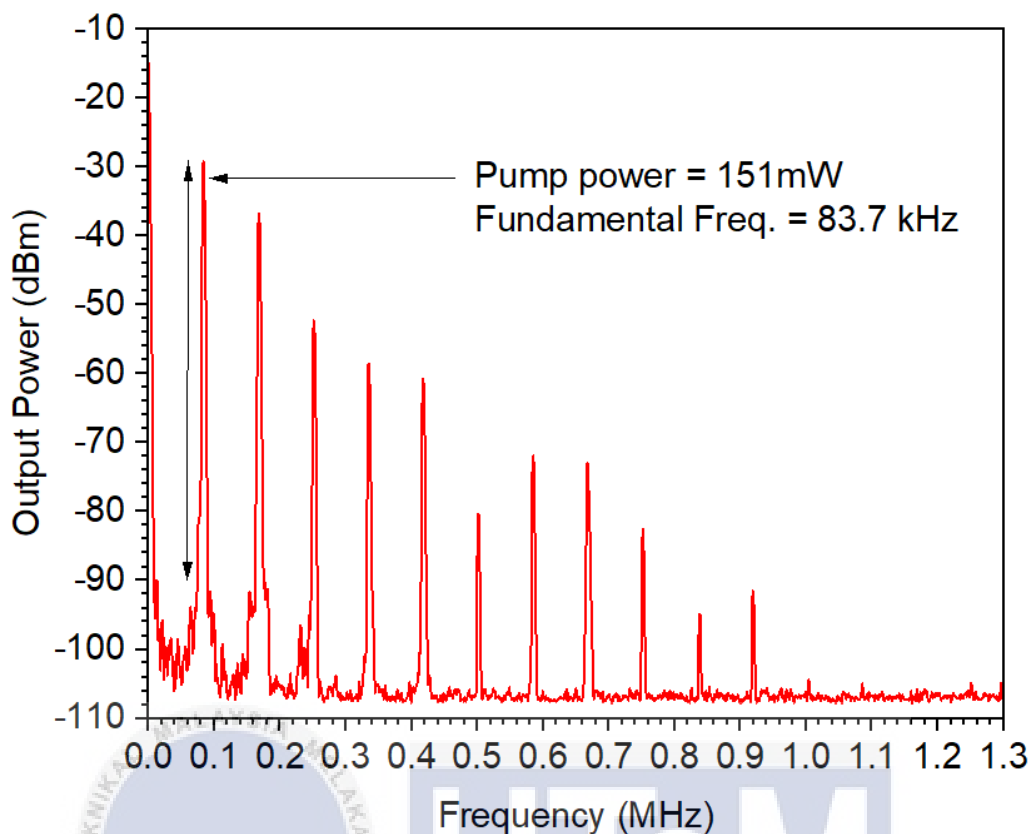


**Figure 4.10: The full span of RF spectrum**

Figure 4.11 demonstrates the signal-to-noise ratio (SNR) is 46 dB, it shows a stable pulsed laser where the SNR is more than 30 dB. The Q-switched laser operates in a stable condition with normal harmonic gradually declines from the left to right within 1.2 MHz of frequency bandwidth.

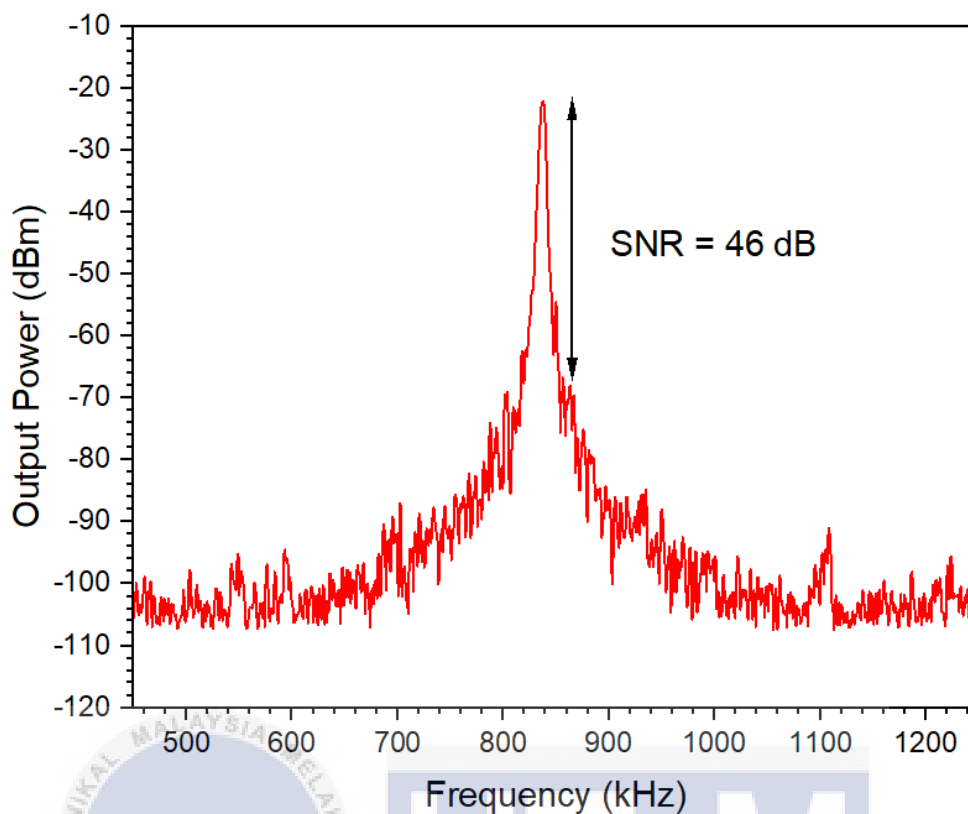


**Figure 4.11: The zoomed image at fundamental frequency of RF spectrum**

Figure 4.12 demonstrates the overall performance of the pulse width and repetition rate against the pump power in Q-switched pulse laser performance. The repetition rate is gradually increasing from 57.74 kHz to 83.70 kHz. Meanwhile, the result of pulse width shows the plotted decreased from 4.27 $\mu$ s to 2.62 $\mu$ s when the pump power starting increase from 81 mW to 151 mW.



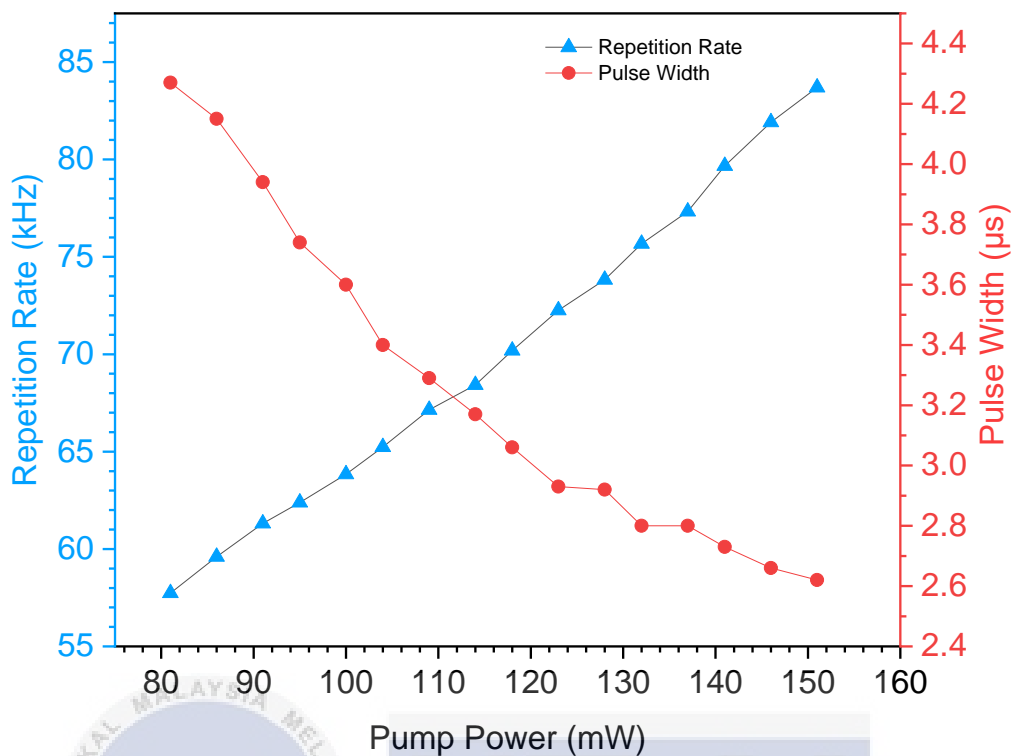


**Figure 4.12: Repetition rate and pulse width as a function of pump power**

The output power, pulse energy, and peak power recorded at various pump power, from 81 mW to 151 mW have been shown in Figure 4.13. The output power is rises from 3.2 to 8.39 mW, which the slope efficiency of output power is 7.09%. Besides, the result of pulse energy can be achieved by the calculation which is the average power divided by the repetition rate. It shows that the pulse energy is increasing from 55.42 nJ to 100.24 nJ. Same with pulse energy, the result of the peak power also came from the calculation which is pulse energy divided by pulse width. The result obtains for peak power based on the obtained data from the pulsed laser performance, it shows the peak power is rise from 12.98 mW to 38.26 mW.

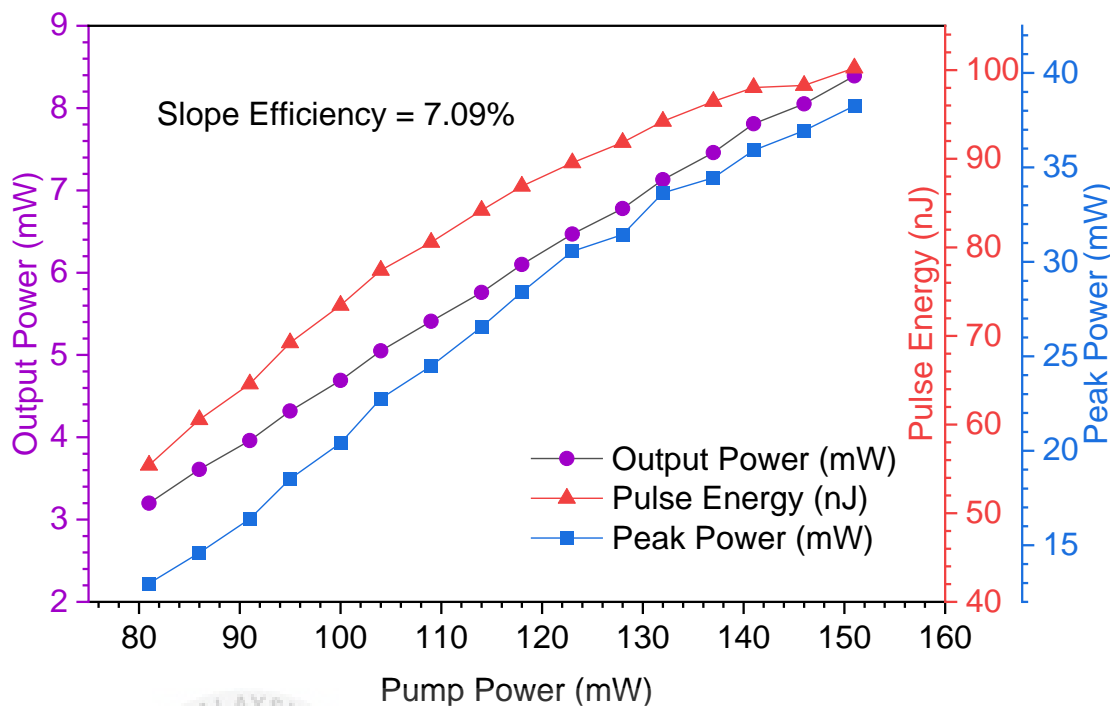


**Figure 4.13: Output power, pulse energy, and peak power as a function of pump power**

#### 4.3 Result Discussion

From the results obtained, the central wavelength was captured at C-band region which is 1533.6 nm at pump power of 151 mW. The peak intensity of Q-switched pulsed laser is  $-2.9$  dBm and 3-dB bandwidth around 3 nm span. The spectrum of continuous-wave lasing was recorded at 1561.8 nm with peak intensity of 2.4 dBm. The RF spectrum at pump power of 151 mW was recorded the fundamental frequency of 83.7 kHz which equivalent to the repetition rate that recorded with digital oscilloscope. The signal-to-noise ratio of the RF spectrum from first peak to bottom signal floor is 46 dB.

Based on preliminary results, the laser performance of  $Ti_4AlN_3$  was aligned with previous research from other researchers. The plotted graph of repetition rate was proportional to the pump power while the result of pulse width was inversely proportional to the pump power. The performance can be seen where the repetition rate was inclined from 57.74 kHz to 83.7 kHz when the pump power increased from 81 mW to 132 mW while the pulse width declined from 4.27  $\mu$ s to 2.62  $\mu$ s. The result of output power, pulse energy, and peak power were directly proportional to the pump power, and it shows that the output power was increased from 3.2 mW to 8.39 mW, the pulse energy rise from 55.42 nJ to 100.24 nJ, and the peak power incline from 12.98 mW to 38.26 mW.

**Table 4.1: Comparison of performance between saturable absorbers**

SAs	Method	Min. Pulse Width ( $\mu$ s)	Max. Repetition Rate (kHz)	Max Output Power (mW)	Max Pulse Energy (nJ)	Ref
Bi <sub>2</sub> Te <sub>3</sub>	D-Shaped Fiber	2.81	42.8	0.6	12.7	[36]
MoS <sub>2</sub>	D-Shaped Fiber	3.19	25.3	0.4	90	[35]
Ti <sub>3</sub> AlC <sub>2</sub>	Thin Film	3.93	112	8.4	75	[37]
Ti <sub>3</sub> AlC <sub>2</sub>	D-Shaped Fiber	2.93	96.15	14.6	151.8	[37]
Ti <sub>4</sub> AlN <sub>3</sub>	D-Shaped Fiber	2.62	83.7	8.4	100.2	[my work]

The table provides a comprehensive overview of different materials, fabrication methods, and their corresponding optical properties comparing with my work MAX phase  $Ti_4AlN_3$ , which contain the method of integration with 4 key parameters to compared among others. As the minimum pulse width represents the shortest duration of a pulse emitted by the laser, it is a critical parameter for applications requiring short and precise pulses. In terms of minimum pulse width,  $Bi_2Te_3$  in a D-shaped fiber configuration exhibits the shortest duration at 2.81  $\mu s$ , implying its efficiency in generating ultra-short pulses. Following closely is  $Ti_4AlN_3$  with a minimum pulse width of 2.62  $\mu s$ , showcasing its capability to produce pulses of similar brevity. In contrast,  $MoS_2$  and Thin Film  $Ti_3AlC_2$  present slightly longer pulse widths at 3.19  $\mu s$  and 3.93  $\mu s$ , respectively, indicating a compromise in achieving the ultra-short pulse durations observed with  $Bi_2Te_3$  and  $Ti_4AlN_3$ .

The maximum repetition rate indicates how quickly pulses can be emitted in succession; it defines the frequency at which pulses are generated. Considering the maximum repetition rate, Thin Film  $Ti_3AlC_2$  stands out with an impressive rate of 112 kHz, suggesting its competence in generating pulses at a very high frequency. It is closely followed by D-shaped fiber  $Ti_3AlC_2$ , demonstrating an exceptional repetition rate of 96.15 kHz.  $Ti_4AlN_3$  shows competitive performance with a maximum repetition rate of 83.7 kHz, indicating its ability to achieve high-frequency pulse generation.  $Bi_2Te_3$  and  $MoS_2$  present lower repetition rates at 42.8 kHz and 25.3 kHz, respectively, suggesting a trade-off between pulse frequency and other performance aspects.

Turning our attention to the maximum output power, maximum output power represents the highest optical power that the laser can deliver. The D-shaped fiber

configuration of Thin Film  $\text{Ti}_3\text{AlC}_2$  boasts an impressive power output of 14.6 mW, indicating its capability to deliver a substantial amount of optical energy. Following closely is D-shaped fiber  $\text{Ti}_4\text{AlN}_3$ , exhibiting a robust maximum output power of 8.4 mW. In comparison, D-shaped fiber  $\text{Bi}_2\text{Te}_3$  presents a lower power output at 0.6 mW, while  $\text{MoS}_2$ , also in a D-shaped fiber setup, shows a maximum power output of 0.4 mW. This highlights the superior power-handling capability of Thin Film  $\text{Ti}_3\text{AlC}_2$  and  $\text{Ti}_4\text{AlN}_3$  in a D-shaped fiber configuration.

Moving on to the maximum pulse energy, it defines the highest amount of energy contained in a single pulse. Thin Film  $\text{Ti}_3\text{AlC}_2$  takes the lead with an impressive 151.8 nJ, showcasing its ability to deliver a substantial amount of energy per pulse. D-shaped fiber  $\text{Ti}_4\text{AlN}_3$  follows closely with a notable pulse energy of 100.2 nJ. In contrast, D-shaped fiber  $\text{Bi}_2\text{Te}_3$  and  $\text{MoS}_2$  present lower maximum pulse energies at 12.7 nJ and 90 nJ, respectively. The variations in maximum pulse energy among these saturable absorbers highlight the importance of considering energy requirements in applications where pulsed fiber lasers are deployed.

For instance, telecommunications that need high repetition rates and short pulse widths are essential for data transmission efficiency. Material processing requires high output power and pulse energy are crucial for efficient material ablation or modification. Medical Applications with short pulse widths and high pulse energy may be important for precision in medical procedures. Considering the trade-offs between these parameters helps researchers and engineers choose the most suitable saturable absorber for their particular laser system and application. The choice of saturable absorber should be driven by the specific demands of the application, balancing considerations of pulse width, repetition rate, output power, and pulse

energy. While  $Ti_3AlC_2$  exhibits superior power and energy characteristics, my MAX phase solution  $Ti_4AlN_3$  as saturable absorber offers a compelling balance between these parameters. The selection depends on the desired trade-offs for a given application, emphasizing the nuanced performance aspects of different saturable absorbers in pulsed fiber laser systems.



## CHAPTER 5

### CONCLUSION AND FUTURE WORKS



## 5.1 Conclusion

The exploration of D-shaped fiber structures coated with 2D materials as saturable absorbers for pulsed fiber lasers has been a transformative journey, driven by two key objectives. The first objective aimed at studying the feasibility of employing D-shaped fiber structures coated with 2D materials as saturable absorbers. The inclusion of MAX phase  $\text{Ti}_4\text{AlN}_3$  in this study was strategically chosen due to its unique combination of metallic and ceramic properties, setting the stage for a comprehensive investigation into its suitability as a saturable absorber.

The project successfully realized the first objective by meticulously studying the fabrication process of D-shaped optical fibers, optimizing them for the incorporation of MAX phase  $\text{Ti}_4\text{AlN}_3$ . The second objective, focusing on the laser performance of 2D material-coated single-mode distributed feedback (SM-DFB) fibers as saturable absorbers, aligns seamlessly with the achievements demonstrated in chapter 3 and 4. Which the MAX phase  $\text{Ti}_4\text{AlN}_3$  achieved the 2.62  $\mu\text{s}$  pulse width, 83.7 kHz repetition rate, 8.4 mW output power, and 100.2 nJ pulse energy.

In-depth analyses of the experimental setup, featuring a ring cavity scheme with a 2.4 m Erbium-doped fiber, a 980 nm laser diode, and the crucial integration of MAX phase  $\text{Ti}_4\text{AlN}_3$  as a saturable absorber, were conducted to fulfil the objectives. The successful generation of Q-switched pulses affirmed the efficacy of MAX phase  $\text{Ti}_4\text{AlN}_3$  in inducing pulsed fiber lasers. These achievements underscore the transformative potential of MAX phase  $\text{Ti}_4\text{AlN}_3$  in advancing the landscape of optical fiber technology.



This study not only presents a thorough exploration of saturable absorbers but also establishes the foundation for future advancements in pulsed fiber laser technology. As we conclude this transformative journey, the successful realization of the objectives illuminates a path forward, indicating the promising role of MAX phase  $\text{Ti}_4\text{AlN}_3$  in the evolution of efficient and innovative fiber laser systems.

## 5.2 Future Works

The success of the current project paves the way for leading future path in the realm of pulsed fiber lasers, particularly those involving MAX phase  $\text{Ti}_4\text{AlN}_3$  as a saturable absorber. A key avenue for future exploration involves the pursuit of generating a mode-locked laser using MAX phase  $\text{Ti}_4\text{AlN}_3$ . This represents an exciting prospect, as mode-locking offers distinct advantages in terms of producing ultrashort pulses and high repetition rates, which are crucial for various applications.

The next phase of research could delve into the optimization of experimental conditions and laser parameters to transition from Q-switched pulses to stable mode-locked operation. This might entail fine-tuning the cavity design, adjusting the pump power, or exploring different configurations to enhance mode-locking capabilities. Comprehensive analyses of the laser's temporal and spectral characteristics during mode-locking operation would provide valuable insights into the behaviour of MAX phase  $\text{Ti}_4\text{AlN}_3$  as a saturable absorber in this distinct regime.

Additionally, future work could focus on the broader integration of MAX phase materials into diverse laser systems, exploring their compatibility with different

wavelengths and gain media. Investigating the scalability of MAX phase  $Ti_4AlN_3$  across various fiber laser architectures and configurations would contribute to a comprehensive understanding of its potential applications.

In conclusion, the future trajectory of this research encompasses the exciting prospect of delving into mode-locking with MAX phase  $Ti_4AlN_3$  as a saturable absorber. This pursuit aligns with the broader goal of advancing the capabilities of pulsed fiber lasers, opening avenues for applications in fields such as telecommunications, medical devices, and industrial processing.



## REFERENCES

- [1] R. Paschotta, article on "Fiber Lasers" in the RP Photonics Encyclopedia, retrieved 2024-01-10.
- [2] Fibers. RP Photonics encyclopedia. url: <https://www.rp-photonics.com/encyclopedia.html>.
- [3] R. Paschotta, article on "Single-mode Fibers" in the RP Photonics Encyclopedia, retrieved 2024-01-10, <https://doi.org/10.61835/2dg>
- [4] Uehara, H., Tokita, S., Kawanaka, J., Konishi, D., Murakami, M., Yasuhara, R.: A passively Q-switched compact Er:Lu<sub>2</sub>O<sub>3</sub> ceramics laser at 2.8  $\mu\text{m}$  with a graphene saturable absorber. *Appl. Phys. Express.* 12(2), 022002 (2019). <https://doi.org/10.7567/1882-0786/aaf994>
- [5] Zhu, G., Zhu, X., Wang, F., Xu, S., Li, Y., Guo, X., Balakrishnan, K., Norwood, R.A., Peyghambarian, N.: Graphene mode-locked Fiber laser at 2.8  $\mu\text{m}$ . *IEEE Photon. Technol. Lett.* 28(1), 7–10 (2019).
- [6] Cao, W.J., Wang, H.Y., Luo, A.P., Luo, Z.C., Xu, W.C.: Graphene-based, 50 nm wide-band tunable passively Q-switched fiber laser. *Laser Phys. Lett.* 9(1), 54–58 (2018).
- [7] Sotor, J., Sobon, G., Krzempek, K., Abramski, K.M.: Fundamental and

harmonic mode-locking in erbium-doped fiber laser based on graphene saturable absorber. *Opt. Commun.* 285(13–14), 3174–3178 (2019).

- [8] Sotor, J., Sobon, G., Abramski, K.M.: Er-doped fibre laser mode-locked by mechanically exfoliated graphene saturable absorber. *Opto–Electron.* 20(4), 362–366 (2019).
- [9] R. Paschotta, article on "Q Switching" in the RP Photonics Encyclopedia, retrieved 2024-01-10, <https://doi.org/10.61835/fdh>
- [10] Maria, L.D., Cennamo, N., Mattiello, F., Chemelli, C., Pesavento, M., Marchetti, S., and Zeni, L. (2017). Analysis of spr sensors in d-shaped pof realized by hand and mechanical polishing. *Multidisciplinary Digital Publishing Institute Proceedings*, 1(8), 767.
- [11] J.D. Zapata D. Steinberg L.A.M. Saito R.E.P. de Oliveira A.M. C´ardenas E.A. Thoroh de Souza. "Efficient graphene saturable absorbers on D-shaped optical fiber for ultrashort pulse generation". In: *Scientific Reports* 6.20644 (2016).
- [12] Liu, X.; Gao, Q.; Zheng, Y.; Mao, D.; Zhao, J. Recent progress of pulsed fiber lasers based on transition-metal dichalcogenides and black phosphorus saturable absorbers. *Nanophotonics* 2020, 9, 2215–2231.
- [13] Wang, G.; Baker-Murray, A.A.; Blau, W.J. Saturable Absorption in 2D Nanomaterials and Related Photonic Devices. *Laser Photonics Rev.* 2019, 13, 1800282.
- [14] Zhang, B.T.; Liu, J.; Wang, C.; Yang, K.J.; Lee, C.; Zhang, H.; He, J.L.O. Recent Progress in 2D Material-Based Saturable Absorbers for All Solid-State

- Pulsed Bulk Lasers. *Laser Photonics Rev.* 2020, 14, 1900240.
- [15] Guo, B.; Xiao, Q.L.; Wang, S.H.; Zhang, H. 2D Layered Materials: Synthesis, Nonlinear Optical Properties, and Device Applications. *Laser Photonics Rev.* 2019, 13, 1800327.
- [16] Zhang, S.; Li, Y.; Zhang, X.; Dong, N.; Wang, K.; Hanlon, D.; Coleman, J.N.; Zhang, L.; Wang, J. Slow and fast absorption saturation of black phosphorus: Experiment and modelling. *Nanoscale* 2018, 8, 17374–17382.
- [17] Li, D.; Jussila, H.; Karvonen, L.; Ye, G.; Lipsanen, H.; Chen, X.; Sun, Z. Polarization and Thickness Dependent Absorption Properties of Black Phosphorus: New Saturable Absorber for Ultrafast Pulse Generation. *Sci. Rep.* 2019, 5, 15899.
- [18] A.R. Muhammad, A.A.A. Jafry, A.M. Markom, A.H.A. Rosol, S.W. Harun, P. Yupapin, Q-Switched YDFL generation by a MAX phase saturable absorber, *Pure Appl. Opt. J. Eur. Opt. Soc. Part A* 59 (2020) 5408–5414.
- [19] A.A.A. Jafry, N. Kasim, M.F.M. Rusdi, A.H.A. Rosol, R.A.M. Yusoff, A.R. Muhammad, B. Nizamani, S.W. Harun, MAX phase based saturable absorber for mode locked erbium-doped fiber laser, *Opt. Laser Technol.* 127 (2020), 106186.
- [20] Park, S., Ruoff, R.S.: Chemical methods for the production of graphenes. *Nat. Nanotechnol.* 4(4), 217–224 (Apr 2019).
- [21] Mohsin Al-Hayali, S.K., Hadi Al-Janabi, A.: Triple-wavelength passively Qswitched ytterbium-doped fibre laser using zinc oxide nanoparticles film as a

- saturable absorber. *J. Mod. Opt.* 65(13), 1559–1564 (2018).
- [22] Chakrabarti, M.H., Manan, N.S.A., Brandon, N.P., Maher, R.C., Mjalli, F.S., AlNashef, I.M., Hajimolana, S.A., Hashim, M.A., Hussain, M.A., Nir, D.: One-pot electrochemical gram-scale synthesis of graphene using deep eutectic solvents and acetonitrile. *Chem. Eng. J.* 274, 213–223 (2018).
- [23] Murdock, A.T., van Engers, C.D., Britton, J., Babenko, V., Meysami, S.S., Bishop, H., Crossley, A., Koos, A.A., Grobert, N.: Targeted removal of copper foil surface impurities for improved synthesis of CVD graphene. *Carbon*. 122, 207–216 (2017).
- [24] Gao, H., Xue, C., Hu, G., Zhu, K.: Production of graphene quantum dots by ultrasound-assisted exfoliation in supercritical CO<sub>2</sub>/H<sub>2</sub>O medium. *Ultrason. Sonochem.* 37, 120–127 (Jul 2017)
- [25] Chia, J.S.Y., Tan, M.T.T., SimKhiew, P., Chin, J.K., Lee, H., Bien, D.C.S., Teh, A.S., Siong, C.W.: Facile synthesis of few-layer graphene by mild solvent thermal exfoliation of highly oriented pyrolytic graphite. *Chem. Eng. J.* 231, 1–11 (2018).
- [26] Yun, W.S., Han, S.W., Hong, S.C., Kim, I.G., Lee, J.D.: Thickness and strain effects on electronic structures of transition metal dichalcogenides: 2HMX<sub>2</sub>semiconductors (M=Mo, W; X=S, Se, Te). *Phys. Rev. B.* 85(3), (2017).
- [27] Xia, H., et al.: Ultrafast erbium-doped fiber laser mode-locked by a CVD-grown molybdenum disulfide (MoS<sub>2</sub>) saturable absorber. *Opt. Express.* 22(14), 17341–17348 (2018).

- [28] Sotor, J., Sobon, G., Abramski, K.M.: Er-doped fibre laser mode-locked by mechanically exfoliated graphene saturable absorber. *Opto-Electron.* 20(4), 362–366 (2017).
- [29] M. Dahlqvist, B. Alling, J. Rosen, Stability trends of MAX phases from first principles, *Phys. Rev. B* 81 (2010) 4.
- [30] J. Lee, S. Kwon, J.H. Lee, Ti<sub>2</sub>AlC-based saturable absorber or passive Q-switching of a fiber laser, *Opt. Mater. Express* 9 (2019) 2057–2066.
- [31] J.J. Feng, X.H. Li, T.C. Feng, Y.M. Wang, J. Liu, H. Zhang, An harmonic mode-locked Er-Doped Fiber laser by the evanescent field-based MXene Ti<sub>3</sub>C<sub>2</sub>T<sub>x</sub> (T = F, O, or OH) saturable absorber, *Ann. Phys.* 532 (2020) 7.
- [32] Y.I. Jhon, J. Koo, B. Anasori, M. Seo, J.H. Lee, Y. Gogotsi, Y.M. Jhon, Metallic MXene saturable absorber for femtosecond mode-locked lasers, *Adv. Mater.* 29 (2017), 1702496.
- [33] D. Mao, X. She, B. Du, D. Yang, W. Zhang, K. Song, X. Cui, B. Jiang, T. Peng, J. Zhao, Erbium-doped fiber laser passively mode locked with few-layer WSe<sub>2</sub>/MoSe<sub>2</sub> nanosheets, *Sci. Rep.* 6 (2017), 23583.
- [34] D. Mao, Y.D. Wang, C.J. Ma, L. Han, B.Q. Jiang, X.T. Gan, S.J. Hua, W.D. Zhang, T. Mei, J.L. Zhao, WS<sub>2</sub> mode-locked ultrafast fiber laser, *Sci. Rep.* 5 (2018) 7.
- [35] Z.Q. Luo, Y.Z. Huang, M. Zhong, Y.Y. Li, J.Y. Wu, B. Xu, H.Y. Xu, Z.P. Cai, J. Peng, J. Weng, 1-, 1.5-, and 2- $\mu$ m Fiber lasers Q-Switched by a broadband few layer MoS<sub>2</sub> saturable absorber, *J. Light. Technol.* 32 (2018) 4077–4084.

- [36] Z.C. Luo, M. Liu, H. Liu, X.W. Zheng, A.P. Luo, C.J. Zhao, H. Zhang, S.C. Wen, W.C. Xu, 2 GHz passively harmonic mode-locked fiber laser by a microfiber-based topological insulator saturable absorber, *Opt. Lett.* 38 (2019) 5212–5215.
- [37] Afiq Arif Aminuddin Jafry, Nabilah Kasim, Bilal Nizamani, Ahmad Razif Muhammad, Rabi'atul Adawiyah Mat Yusoff, Sulaiman Wadi Harun, Preecha Yupapin, MAX phase  $Ti_3AlC_2$  embedded in PVA and deposited onto D-shaped fiber as a passive Q-switcher for erbium-doped fiber laser, *optik* 224 (2020) 165682.

